Translating GWAS-identified loci for cardiac rhythm and rate using an *in vivo* image- and CRISPR-Cas9-based approach

Benedikt von der Heyde[1,2], Anastasia Emmanouilidou[1,2], Tiffany Klingström[1,2], Eugenia Mazzaferro[1,2], Silvia Vicenzi[1,2], Sitaf Jumaa[1,2], Olga Dethlefsen[3,4], Harold Snieder[5], Eco de Geus[6], Erik Ingelsson[2,7,8,9], Amin Allalou[2,10], Hannah L. Brooke[11], Marcel den Hoed[#1,2]

[1]The Beijer laboratory and Department of Immunology, Genetics and Pathology, Uppsala University, Uppsala, Sweden.
[2]Science for Life Laboratory, Uppsala University, Uppsala, Sweden.
[3]Science for Life Laboratory, Stockholm University, Stockholm, Sweden.
[4]National Bioinformatics Infrastructure Sweden, Stockholm University, Stockholm, Sweden.
[5]Department of Epidemiology, University of Groningen, University Medical Center Groningen, Groningen, the Netherlands.
[6]Department of Biological Psychology, Vrije Universiteit Amsterdam, Amsterdam, the Netherlands.
[7]Department of Medical Sciences, Molecular Epidemiology, Uppsala University, Uppsala, Sweden.
[8]Department of Medicine, Division of Cardiovascular Medicine, Stanford University School of Medicine, Stanford, CA, USA.
[9]Stanford Cardiovascular Institute, Stanford University, Stanford, CA 94305.
[10]Department of Information Technology, Division of Visual Information and Interaction, Uppsala University, Uppsala, Sweden.
[11]Department of Public Health and Caring Sciences, Uppsala University, Uppsala, Sweden.

Corresponding author: Marcel den Hoed

Abstract

A meta-analysis of genome-wide association studies (GWAS) identified eight loci that are associated with heart rate variability (HRV) in data from 53,174 individuals. However, functional follow-up experiments - aiming to identify and characterize causal genes in these loci - have not yet been performed. We developed an image- and CRISPR-Cas9-based pipeline to systematically characterize candidate genes for HRV in live zebrafish embryos and larvae. Nine zebrafish orthologues of six human candidate genes were targeted simultaneously in fertilized eggs from fish that transgenically express GFP on smooth muscle cells (Tg(*acta2:GFP*)), to visualize the beating heart using a fluorescence microscope. An automated analysis of repeated 30s recordings of 381 live zebrafish atria at 2 and 5 days post-fertilization highlighted genes that influence HRV (*hcn4* and *si:dkey-65j6.2*); heart rate (*rgs6 and hcn4*) and the risk of sinoatrial pauses and arrests (*hcn4*). Hence, our screen confirmed the role of established genes for heart rate and rhythm (*rgs6* and *hcn4*), and highlighted a novel gene implicated in HRV (*si:dkey-65j6.2*).

Introduction

Heart rate variability (HRV) reflects the inter-beat variation of heart rate. HRV is controlled by the sinoatrial node, which receives input from the autonomic nervous system. Autonomic imbalance has been associated with work stress and other modifiable or non-modifiable risk factors[1], and is reflected in lower HRV. Lower HRV has been associated with higher cardiac morbidity and mortality[2], and with a higher risk of all-cause mortality[3]. HRV can be quantified non-invasively using the RR interval of a 12-lead ECG, making HRV a useful clinical marker for perturbations of the autonomic nervous system. However, the genetic basis of HRV remains largely elusive.

Recently, we and others identified the first loci that are robustly associated with HRV, using a meta-analysis of genome-wide association studies (GWAS) with data from 53,174 participants[4]. Eleven of the 17 associated single nucleotide polymorphisms (SNPs) overlapped with loci that are also associated with resting heart rate[5]. The heart rate associated loci in turn had on aggregate been associated with altered cardiac conduction and risk of sick sinus syndrome[5]. *In silico* functional annotation of the five loci that are associated with both HRV[6] and heart rate[5] previously resulted in the prioritization of six candidate genes that are anticipated to be causal[6]. Functional follow-up experiments - ideally *in vivo* - are required to conclude if these genes are indeed causal, and examine if they influence HRV, heart rate, and/or cardiac conduction.

Mouse models are commonly used in cardiac research, but mice show substantial differences in cardiac rate and electrophysiology when compared with humans[7]. Inherently, these differences complicate extrapolation of results from mouse models to humans[7]. Additionally, rodents are not suitable for high-throughput, *in vivo*

72 characterization of cardiac rhythm and rate. Such screens are essential to
73 systematically characterize positional candidate genes in the large number of loci that
74 have now been identified by GWAS for cardiac rhythm[4], rate[8] and conduction[9].
75 Hence, novel model systems that facilitate systematic, *in vivo* characterization of a
76 large number of candidate genes are desirable.

77 In recent years, the zebrafish has become an important model system for genetic
78 and drug screens for human disease[10,11]. Despite morphological differences to the
79 human heart, zebrafish have a functional, beating heart at ~24 hours post-fertilization,
80 and the ECG of the two-chambered zebrafish heart is similar to that of humans[12].
81 Conditions affecting cardiac electrophysiology have previously been successfully
82 modeled in zebrafish. For example *nkx2.5* has been demonstrated to be necessary for
83 establishing HRV[13], mutations in *kcnh2* were used to model long QT syndrome[14],
84 *trpm7* was shown to influence heart rate and risk for sinoatrial pauses[15], and *hcn4*
85 knockdown modeled sick sinus syndrome in zebrafish analogous to the human
86 condition[16]. Fluorescently labeled transgenes facilitate visualization of cell types and
87 tissues of interest, which can now be accomplished in high-throughput thanks to
88 advances in automated positioning of non-embedded, live zebrafish embryos[17]. The
89 automated positioning system has already been used to identify and characterize small
90 molecules for myelination[18] and thyroid disease[19]. In addition, the zebrafish has a
91 well-annotated genome, with orthologues of at least 71.4% of human genes[20]. These
92 genes can be targeted efficiently and in a multiplexed manner thanks to recent
93 advances in Clustered, Regulatory Interspaced, Short Palindromic Repeats (CRISPR)
94 and CRISPR-associated systems (Cas)[21]. All characteristics combined make zebrafish
95 embryos and larvae an attractive model system to systematically characterize
96 candidate genes for cardiac rhythm, rate and conduction.

97 The aim of this study was to objectively characterize the most promising candidate
98 genes in GWAS-identified loci for HRV as well as heart rate for a role in cardiac
99 rhythm, rate and function using a large-scale, image-based screen in zebrafish
100 embryos and larvae.
101

Results

Descriptive results

At 2dpf, some embryos showed sinoatrial pauses (n=39, 10.3%**,** Supplementary Movie 1) and arrests (n=36, 9.5%, Supplementary Movie 2); cardiac edema (n=16, 4.2%); or uncontrolled atrial contractions (n=1, 0.2%, Supplementary Movie 3). Three larvae died between 2 and 5dpf (Supplementary Figure 1). At 5dpf, fewer larvae displayed sinoatrial pauses (n=9, 2.7%, one of which had a sinoatrial pause at 2dpf); sinoatrial arrests (n=3, 0.9%, none of which had a sinoatrial arrest at 2dpf); and cardiac edema (n=15, 4.5%, nine of which had an edema at 2dpf); while more larvae showed uncontrolled atrial contractions (n=9, 2.7%, none of which had uncontrolled atrial contraction at 2dpf); or an abnormal cardiac morphology and impaired cardiac contractility (n=6, 1.8%, Supplementary Movie 4).

After imaging at 5dpf, all larvae were sequenced at the nine CRISPR-Cas9 targeted sites (Figure 1, Table 1), as well as at three *in silico* predicted off-target sites (Supplementary Table 1). Transcript-specific dosages were calculated by weighting the number of mutated alleles by their predicted impact on protein function based on Ensembl's variant effect predictor (VEP). No CRISPR-Cas9 induced mutations were identified at any of the predicted off-target sites (Supplementary Table 2). A total of 169 unique mutations were identified across the nine CRISPR-targeted sites, ranging from three unique mutations in *hcn4l* to 34 in *si:dkey-65j6.2* (i.e. *KIAA1755*) (Supplementary Table 3). Frameshift mutations were most common (47.9%), followed by missense variants (25.4%), in-frame deletions (14.2%), and synonymous variants (5.9%). Eighty-seven, seventy-two and ten variants were predicted to have a high, moderate, and low impact on protein function, respectively (Supplementary

126 Table 3). Mutant allele frequencies ranged from 4.1% for *hcn4l* to 93.4% for *neo1b*
127 (Supplementary Table 4).

128 *Genetic effects on cardiac rhythm and rate*

129 Each additional mutated allele in *rgs6* was associated with a lower heart rate at 2dpf,
130 independently of HRV (Figure 2, Supplementary Table 5). Larvae with CRISPR-
131 induced mutations in *rgs6* were shorter at 2 and 5 dpf, and had a smaller dorsal area at
132 5dpf (Supplementary Figure 2, Supplementary Table 6). These results were mostly
133 driven by heterozygous larvae, since only one larva carried two mutated *rgs6* alleles
134 (Supplementary Table 4).

135 At 2dpf, *hcn4* influenced heart rate independently of HRV when larvae with two
136 functionally knocked alleles were compared with wildtypes (Supplementary Table 7),
137 and may affect HRV when adjusting for heart rate (Supplementary Table 5).
138 Furthermore, *hcn4*-affected embryos had higher odds of a sinoatrial pause or arrest at
139 2dpf (Table 2, Supplementary Table 8). At 5dpf, *hcn4* affected heart rate as well as
140 HRV, with effect sizes attenuated but not abolished when adjusting for the other trait
141 (Supplementary Table 5,7). The odds of a sinoatrial arrest was similar at 5dpf
142 compared with 2dpf, but did not reach significance at 5dpf (Supplementary Table 8).

143 Each additional mutated allele in the main transcript of *si:dkey-65j6.2* (i.e.
144 *KIAA1755*) tended to be associated with a higher HRV at 2dpf as well as at 5dpf
145 (Figure 2, Supplementary Table 5). Additionally, *si:dkey-65j6.2*-affected larvae
146 tended to be smaller at 2 and 5dpf (Supplementary Figure 2, Supplementary Tables 6,
147 9). Larvae with mutations in *quo* (i.e. the other *KIAA1755* orthologue) were larger at 2
148 and 5dpf (Supplementary Figure 2, Supplementary Tables 6, 9).

149 Larvae with two vs. zero functionally knocked *syt10* alleles tended to have a higher
150 odds of sinoatrial pauses at 2 and 5dpf (Supplementary Tables 8, 10).

151 Larvae with mutations in *neo1a* tended to be larger at 2dpf (Supplementary Figure

152 2, Supplementary Tables 6, 9).

153

154 **Discussion**

155 Large-scale, *in vivo* follow-up studies of candidate genes in GWAS-identified loci
156 remain sparse. Here we present an objective, image-based pipeline to systematically
157 characterize candidate genes for cardiac rhythm, rate, and conduction-related
158 disorders. Using a zebrafish model system, we confirmed the roles of genes
159 previously implicated in heart rate and rhythm (*rgs6* and *hcn4*), provided a novel gene
160 influencing cardiac rhythm (*si:dkey-65j6.2*, i.e. *KIAA1755*), and observed an effect of
161 previously unanticipated genes on early growth and development (*rgs6*, *quo*, *si:dkey-*
162 *65j6.2*, *neo1a*). Additionally, we confirmed that knockdown of *hcn4* results in
163 sinoatrial pauses[16]. These results add weight to the notion that GWAS-identified
164 common variants for complex traits can flag genes for which rare, detrimental
165 mutations cause severe, early-onset disorders[9,22,23]. We show here that systematic
166 characterization of candidate genes in GWAS-identified loci for complex traits using
167 an image- and CRISPR-Cas9-based zebrafish model system can help identify
168 clinically relevant causal genes, and aid confirmation of the role of such genes in
169 whole-exome sequencing efforts in humans by reducing the multiple testing burden[24].

170 Regulator of G protein signaling 6 (RGS6) plays a role in the parasympathetic
171 regulation of heart rate[28] and is a negative regulator of muscarinic signaling, thus
172 decreasing HRV to prevent bradycardia. Common variants near *RGS6* have been
173 identified in GWAS for resting heart rate[8,25,26], heart rate recovery after exercise[27] and
174 HRV[4]. An eQTL analysis using GTEx data showed that the minor T-allele in
175 rs4899412 that is associated with lower HRV is also associated with a higher
176 expression of *RGS6* in esophagus and tibial nerve. This is directionally consistent
177 with humans with loss-of-function variants in *RGS6* showing higher heart rate
178 variability[29]. Also in line with this, mice deficient in *Rgs6* (*Rgs6*$^{-/-}$) were previously

179 characterized by bradycardia, higher HRV and susceptibility to atrioventricular
180 block[30]. In our study, zebrafish embryos with CRISPR-induced mutations in *rgs6* had
181 a lower heart rate at 2dpf, independently of HRV. Hence, our results for heart rate are
182 in line with studies in murine models. However, we did not detect an effect of
183 mutations in *rgs6* on HRV in our study, possibly due to the low mutant allele
184 frequency of *rgs6*.

185 The locus harboring *HCN4* has been identified in GWAS for HRV[6], heart rate[5] and
186 atrial fibrillation[31]. *HCN4* is arguably the most well characterized gene in the context
187 of cardiac rhythm. It belongs to the family of "funny" channels, aptly named for being
188 activated upon hyperpolarization and non-selective permeability by Na^+ and K^+. It is
189 expressed in the sinoatrial node[32,33] and plays an important role in cardiac pace
190 making[34]. The heart rate lowering agent ivabradine[35] is an open channel blocker of
191 *HCN4*, and reduces cardiovascular and all-cause mortality in heart failure patients[36].
192 *Hcn4*$^{-/-}$ mice die prenatally, and analyses of their hearts show no arrhythmias and a
193 lower heart rate compared with wildtype and heterozygotes[34]. In line with this,
194 humans that are heterozygous for an *HCN4* loss of function mutation are typically
195 characterized by bradycardia. Comparably, knockdown of *hcn4* in zebrafish using
196 morpholinos resulted in bradycardia and sinoatrial pauses[16]. We identified nine
197 zebrafish embryos that were compound heterozygous for mutations that result in a
198 functional knock of *hcn4*, and one embryo that was compound heterozygous for such
199 mutations in *hcn4l*. Mutations in both orthologues did not deviate from HWE
200 (Supplementary Table 4). Four of the nine compound heterozygous larvae for *hcn4*,
201 and four of the eight larvae that were heterozygous for mutations in *hcn4* as well as
202 *hcn4l* showed a sinoatrial arrest before the atrial recording was initiated at 2dpf.
203 Zebrafish embryos can survive without a functional heart at this stage, thanks to

204 adequate tissue oxygenation by diffusion[37]. This allowed us to witness genetically
205 driven cardiac arrests that would have been lethal in embryos of other species.
206 However, the direction of effect on heart rate that we observed is unexpected. It most
207 likely reflects overcompensation by *hcn4l*, or another gene that has been induced by
208 *hcn4* knockout[38]. We cannot rule out that some of the CRISPR-Cas9 induced
209 mutations represent a gain-of-function either. Our gRNA binds in the first exon of
210 *hcn4*, and cuts in the vicinity of the ion-transport domain, as annotated by protein
211 families (PFAM)[39]. A gain-of-function variant was identified in humans that
212 increased *HCN4*'s susceptibility to cAMP[40]. In line with this, overexpression of *Hcn4*
213 in mice resulted in lower HRV[41]. Hence, we may have induced an *hcn4* gain-of-
214 function mutation in a subset of the larvae.

215 Non-synonymous SNPs in *KIAA1755* have been identified in GWAS for HRV[6]
216 and heart rate[5]. In our analysis, *si:dkey-65j6.2*-affected larvae have a higher HRV at 2
217 and 5dpf, largely independently of heart rate. In humans, the C-allele of the HRV-
218 associated rs6123471 in the 3' UTR of *KIAA1755* is associated with a lower
219 expression of *KIAA1755* in brain and aorta (GTEx[42]), a higher HRV[6], and a lower
220 heart rate[5]. Hence, a higher HRV at 2 and 5dpf for each additional mutated allele in
221 *si:dkey-65j6.2* is directionally consistent with results in humans. Genetic effects on
222 HRV and heart rate were mutually adjusted in our sensitivity analysis, which may
223 have revealed the unbiased direction of effect for mutations in *KIAA1755* on HRV. In
224 other words: the GWAS-identified association of the *KIAA1755* locus - and possibly
225 other loci - with heart rate may have been driven by HRV. This would explain why
226 the eleven HRV-associated loci that showed evidence of an association with heart rate
227 all did so in the expected (i.e. opposite) direction from a phenotypic point of view[6].
228 *KIAA1755* is a previously uncharacterized gene that shows a broad expression pattern,

229 including different brain regions and the left atrial appendage (GTEx[42]). Future
230 mechanistic studies are required to distill how *KIAA1755* influences heart rhythm.

231 *SYT10* belongs to the family of synaptogamins: transmembrane proteins that are
232 involved in regulation of membrane trafficking in neurons[43], which is important for
233 neurotransmitter release[44]. Variants in or near *SYT10* have previously been associated
234 with HRV[6] as well as with heart rate [5] and heart rate recovery[27]. Since *SYT10* is
235 mainly expressed in brain, tibial nerve and pituitary (GTEx[42]). The trend towards
236 higher odds of sinoatrial pauses in larvae with CRISPR-induced mutations in *syt10*
237 may be mediated by altered neurotransmitter release.

238 In addition to the additive analysis, we were able to compare embryos and larvae
239 with two functionally knocked out alleles with wildtypes for six out of nine orthologs.
240 These analyses largely confirmed the association of the additive analysis, but also
241 revealed novel associations. Screening the F_0 or F_2 generation instead would have had
242 their own advantages and disadvantages. Wu and colleagues described a powerful
243 approach to efficiently disrupt and analyze F_0 larvae[45]. However, this approach
244 requires sham injected controls, and is not compatible with multiplexing of many
245 gRNAs. Hence, we argue that non-conclusive results for a subset of candidate genes
246 in the screen is not problematic when systematically characterizing a large number of
247 candidate genes.

248 The large differences in mutant allele frequency across target genes can be
249 attributed to several factors. First, the mosaic founders were in-crossed six times,
250 while random mating was allowed. Hence, we did not ascertain which fish generated
251 the offspring in each mating. Secondly, while all gRNAs were pre-tested, mutated
252 alleles that didn't affect the germline were not included in our screen. Thirdly, larvae
253 that carry embryonic lethal variants were not included in the screen.

254 Four limitations of our study should be discussed. Firstly, acquiring 30s recordings
255 implies that false negatives for sinoatrial pauses or arrests are inevitable. We decided
256 to exclude the 54 embryos and eight larvae with a sinoatrial pause or arrest during
257 positioning for imaging from the analysis, because the case status of these samples
258 cannot be confirmed objectively; yet they are not appropriate controls either. This
259 limitation will have resulted in conservative effect estimates for sinoatrial pauses and
260 arrests. Secondly, CRISPR guide-RNAs with predicted off-target effects free from
261 mismatches were avoided. However, two of the selected targets - i.e. for *hcn4* and
262 *si:dkey-65j6.2* - had predicted exonic off-targets with three mismatches at the time we
263 designed the gRNAs (Supplementary Table 1). Human orthologues of potential off-
264 target genes *dclk1* and *galnt10* have previously been associated with heart rate
265 variability-related traits[46] (*dclk1*), as well as with carotid intima-media thickness[47] and
266 body mass index[48-50] (*galnt10*). However, sequencing larvae at the three predicted off-
267 target regions did not show any CRISPR-Cas9 induced mutations (Supplementary
268 Table 2). In line with predictions by Varshney *et al*., off-target effects are thus
269 unlikely to have influenced our results[51]. We cannot exclude the possibility of there
270 being other, non-predicted off-target effects though. Thirdly, we in-crossed mosaic
271 founder mutants (F_0) and phenotypically screened and sequenced the F_1 generation.
272 For some genes, this yielded a small number of larvae with 0 or 2 mutated alleles (i.e.
273 for *rgs6*, *hcn4*, and *hcn4l*), resulting in a lower statistical power to find true genetic
274 effects - if present - for these genes. In spite of this limitation, we were able to detect
275 significant effects of mutations in *rgs6* and *hcn4*. Finally, we recorded the atrium
276 only, to enable a higher frame rate, a higher resolution in time for HRV, and a higher
277 statistical power to detect small genetic effects on HRV. As a result, any ventricular
278 abnormalities were not registered, and uncontrolled atrial contractions may thus

279 reflect atrial fibrillation, premature atrial contractions, high atrial rate, or atrial
280 tachycardia.

281 Strengths of our study include its repeated measures design, which enabled us to
282 capture genetic effects at different stages of early development in zebrafish.
283 Furthermore, the throughput of the setup allowed us to examine the effect of multiple
284 genes simultaneously, in an unprecedented sample size for *in vivo* genetic screens.
285 Our results demonstrate that a large sample size is paramount to robustly detect
286 genetic effects on complex traits in zebrafish embryos and larvae when screening the
287 F_1 generation, even for functional knockout mutations. Identifying CRISPR-Cas9-
288 induced mutations allele-specifically using a custom-written algorithm helped us
289 classify larvae as heterozygous and compound heterozygous, which in turn helped
290 pinpoint the true effect of mutations in these genes. Also, our study is based on a
291 high-throughput imaging approach with objective, automated quantification, as
292 compared with more manual annotation of previous studies[5]. Finally, for all genes that
293 showed an effect on HRV, directions of effect were directionally consistent with
294 eQTL associations in humans. This further emphasizes the strength of our model
295 system and the robustness of our findings.

296 In conclusion, our large-scale imaging approach highlights that zebrafish embryos
297 and larvae can be used for rapid and comprehensive follow-up of GWAS-prioritized
298 candidate genes. This will likely increase our understanding of the underlying biology
299 of heart rate and rhythm, and potentially yield novel drug targets.

300

301 **Methods**

302 *Candidate gene selection*

303 Candidate genes in GWAS-identified loci for HRV were identified as described in
304 detail in Nolte et al.[4]. Of the 18 identified candidate genes, six were selected for
305 experimental follow-up. This selection was based on overlap with findings from
306 GWAS for heart rate (*KIAA1755*, *SYT10*, *HCN4*, *GNG11*)[5], as well as with results
307 from eQTL analyses in sinoatrial node and brain (*RGS6*). Additional candidate genes
308 from the same or nearby loci were also selected for experimental follow-up, i.e.
309 *NEO1*, which resides next to *HCN4*. Zebrafish orthologues of the human genes were
310 identified using Ensembl, as well as using a comprehensive synteny search using
311 Genomicus[52] (Supplementary Table 1). Of the selected genes, *GNG11*, *SYT10* and
312 *RGS6* have one orthologue in zebrafish, and *KIAA1755*, *HCN4* and *NEO1* each have
313 two orthologues, resulting in a total of nine zebrafish orthologues for six human
314 candidate genes (Table 1).

315

316 *Mutagenesis*

317 All nine zebrafish genes were targeted together using a multiplexed CRISPR-Cas9
318 approach described recently[21]. Briefly, guide-RNAs (gRNAs) were selected using
319 ChopChop[53] and CRISPRscan[54] (Supplementary Table 1), based on their predicted
320 efficiency, a moderate to high GC-content, location in an early exon, and absence of
321 predicted off-target effects without mismatches. Oligonucleotides were designed as
322 described[21], consisting of a T7 or SP6 promotor sequence (for gRNAs starting with
323 'GG' or 'GA', respectively), a gene-specific gRNA-target sequence, and an overlap
324 sequence to a generic gRNA. The gene-specific oligonucleotides were annealed to a

325 generic 80 bp long oligonucleotide at 98°C for 2 mins, 50°C for 10 mins, and 72°C
326 for 10 mins. The products were checked for correct length on a 2% agarose gel. The
327 oligonucleotides were subsequently transcribed *in vitro* using the manufacturer's
328 instructions (TranscriptAid T7 high yield transcription kit / MEGAscript SP6
329 transcription kit, both ThermoFisher Scientific, Waltham, USA). The gRNAs were
330 purified, after which the integrity of the purified gRNAs was examined on a 2%
331 agarose gel. The zebrafish codon-optimized plasmid pT3TS-nls-zCas9-nls was used
332 as a template to produce Cas9 mRNA[55]. The plasmid was linearized with Xba1, and
333 then purified using the Qiaprep Spin Miniprep kit (Qiagen, Hilden, Germany). The
334 DNA was transcribed using the mMESSAGE mMACHINE T3 Transcription Kit
335 (ThermoFisher Scientific, Waltham, USA), followed by LiCl precipitation. The
336 quality of the RNA was confirmed on a 1% agarose gel.

337

338 *Husbandry & microinjections*

339 A zebrafish line with GFP-labelled α-smooth muscle cells Tg(*acta2*:GFP)[56] was used
340 to visualize the beating heart. To this end, eggs from an in-cross of Tg(*acta2*:GFP)
341 fish were co-injected with a mix of Cas9 mRNA (final concentration 150 ng/µl) and
342 all nine gRNAs (final concentration 25 ng/µl each) in a total volume of 2nL at the
343 single-cell stage. CRISPR-Cas9 injected embryos were optically screened for the
344 presence of Tg(*acta2*:GFP) at 2 days post fertilization (dpf), using an automated
345 fluorescence microscope (EVOS FL Cell imaging system, ThermoFisher Scientific,
346 Waltham, USA). Tg(*acta2*:GFP) carriers were retained and raised to adulthood in
347 systems with circulating, filtered and temperature controlled water (Aquaneering, Inc,
348 San Diego, CA). All procedures and husbandry were conducted in accordance with

349 Swedish and European regulations, and have been approved by the Uppsala
350 University Ethical Committee for Animal Research (C142/13 and C14/16).

351

352 *Experimental procedure imaging*

353 The mosaic founder mutants (F_0 generation) were only used for reproduction. After
354 crossing the founder mutants, F_1 embryos were used for experiments. To reach the
355 experimental sample size, founder mutants were incrossed six times. At all occasions,
356 mating was entirely random. Eggs were collected after F_0 fish were allowed to
357 reproduce for 45 mins to minimize variation in developmental stage. Fertilized eggs
358 were placed in an incubator at 28.5°C. At 1dpf, embryos were dechorionated using
359 pronase (Roche Diagnostics, Mannheim, Germany).

360 At 2dpf, embryos were removed from the incubator and allowed to adapt to controlled
361 room temperature (21.5 °C) for 20 mins. Individual embryos were exposed to 100
362 µg/ml Tricaine (MS-222, Sigma-Aldrich, Darmstadt, Germany) for 1 min before
363 being aspirated, positioned in the field of view of a fluorescence microscope, and
364 oriented dorsally using a Vertebrate Automated Screening Technology (VAST)
365 BioImager (Union Biometrica Inc., Geel, Belgium). We subsequently acquired twelve
366 whole-body images, one image every 30 degrees of rotation, using the camera of the
367 VAST BioImager to quantify body length, dorsal and lateral surface area and volume,
368 as well as the presence or absence of cardiac edema. The VAST BioImager then
369 positioned and oriented the larva to visualize the beating atrium and triggered the
370 upright Leica DM6000B fluorescence microscope to start imaging using a HCX APO
371 L 40X/0.80 W objective and L5 ET, k filter system (Micromedic AB, Stockholm,
372 Sweden). Images of the beating atrium were acquired for 30s at a frame rate of 152

373 frames/s using a DFC365 FX high-speed CCD camera (Micromedic AB, Stockholm,
374 Sweden). After acquisition, the larvae were dispensed into a 96-well plate, rinsed
375 from tricaine, and placed back into the incubator. The procedure was repeated at 5dpf
376 (i.e. the larval stage), to allow genetic effects that influence HRV and heart rate
377 differently at different stages of development to be captured[57]. After imaging at 5dpf,
378 the larvae were once again dispensed into 96-well plates, sacrificed, and stored at -
379 80°C for further processing.

380

381 *Quantification of cardiac traits and body size*

382 A custom-written MATLAB script was used to convert the images acquired by the
383 CCD camera into quantitative traits. To acquire the heart rate, each frame of the
384 sequence was correlated with a template frame. The repeating pattern yields a
385 periodic graph from the correlation values and by detecting the peaks in the graph we
386 can assess the heart rate. The template frame should represent one of the extreme
387 states in the cardiac cycle, i.e. end-systole or end-diastole. To detect these frames, we
388 examined the correlation between the first 100 frames. The combination of frames
389 that showed the lowest correlation corresponded to the heart being in opposite states.
390 One of these frames was chosen as the template [58].

391 This numeric information was subsequently used to quantify: 1) heart rate as the
392 inverse of RR-interval; 2) the standard deviation of the normal-to-normal RR interval
393 (SDNN); and 3) the root mean square of successive heart beat interval differences
394 (RMSSD). Finally, a graph of pixel changes over time was generated across the 30s
395 recording to help annotate the script's performance. The files containing the inter-
396 beat-intervals were used to objectively quantify sinoatrial pauses (i.e. the atrium stops

397 beating for longer than 3x the median inter-beat-interval of the larva, Supplementary
398 Movie 1) and sinoatrial arrests (i.e. the atrium stops beating for longer than 2s,
399 Supplementary Movie 2) using a custom-written Stata script. The graphs of pixel
400 changes over time were also used to identify larvae with other abnormalities in
401 cardiac rhythm. Such abnormalities were annotated as: uncontrolled atrial
402 contractions (Supplementary Movie 3); abnormal cardiac morphology (i.e. a tube-like
403 atrium, Supplementary Movie 4); or impaired cardiac contractility (i.e. a vibrating
404 rather than a contracting atrium, Supplementary Movie 4). These phenotypes were
405 annotated independently by two investigators (B.v.d.H. and M.d.H.), resulting in an
406 initial concordance rate >90%. Discrepancies in annotation were discussed and re-
407 evaluated to reach consensus.

408 Bright-field images of the larvae were used to assess body length, dorsal and lateral
409 surface area, and volume. Images were automatically segmented and quantified using
410 a custom-written CellProfiler[59] pipeline, followed by manual annotation for
411 segmentation quality. Larvae with suboptimal segmentation quality due to the
412 presence of an air-bubble, a bent body, an incomplete rotation within the capillary,
413 partial capturing of the larva, or an over-estimation of size were replaced by images
414 with a 180° difference in rotation, or excluded if that image was also sub-optimally
415 segmented. The larva was excluded from the analysis for body volume if more than
416 four of the 12 images had a bad segmentation. Imaging, image quantification and
417 image quality control were all performed blinded to the sequencing results.

418

419

420

421 *Quality control of phenotype data*

422 A series of quality control steps was performed to ensure only high-quality data was
423 included in the genetic association analysis (Supplementary Fig. 1). First, graphs
424 indicating that one or more true beats were missed by the script were removed from
425 the analysis *a priori* (Supplementary Fig. 1). Second, embryos and larvae showing
426 uncontrolled atrial contractions, sinoatrial pauses or arrests, edemas, abnormal
427 morphology and/or reduced contractility, and embryos/larvae annotated to have a
428 sinoatrial pause while positioning before video acquisition were excluded from the
429 analyses for HRV and heart rate (Supplementary Fig. 1). Third, genetic effects on
430 sinoatrial pauses and arrests were examined at 2dpf and 5dpf. For the remainder of the
431 cardiac abnormalities, too few cases were observed to justify a separate association
432 analysis. Furthermore, embryos and larvae that showed a sinoatrial pause or arrest in
433 between positioning and video acquisition, but not during the recording, were
434 excluded from the analysis for sinoatrial pauses and arrests, since we cannot ascertain
435 case status in the same rigorous manner for such samples, but they are not appropriate
436 controls either.

437

438 *Sample preparation for sequencing*

439 After imaging at 5dpf, larvae were sacrificed and DNA was extracted by exposure to
440 lysis buffer (10mM Tris-HCl pH8, 50mM KCl, 1mM EDTA, 0.3% Tween 20, 0.3%
441 Igepal) and proteinase K (Roche Diagnostics, Mannheim, Germany) for 2 h at 55°C,
442 followed by 10 min at 95°C to deactivate the proteinase K. Gene-specific primers
443 (150bp-300bp) amplifying gRNA-targeted and putative off-target regions in *dclk1b*
444 and both *galnt10* orthologues (Supplementary Table 1) were distilled from

445 ChopChop[53] and Primer3[60], and Illumina adaptor-sequences were added.
446 Additionally, we included 96 uninjected Tg(*acta2*:*GFP*) larvae for sequencing across
447 all gene-specific regions to adjust for natural occurring polymorphisms. The first PCR
448 was conducted by denaturation at 98°C for 30s; amplification for 35 cycles at 98°C
449 for 10s, 62°C for 30s and 72°C for 30s; followed by a final extension at 72°C for 2
450 mins. Amplified PCR products were cleaned using magnetic beads (Mag-Bind PCR
451 Clean-up Kit, Omega Bio-tek Inc. Norcross, GA). The purified products were used as
452 a template for the second PCR, in which Illumina Nextera DNA library sequences
453 were attached to allow multiplexed sequencing of all CRISPR-targeted sites across
454 384 larvae in a single lane. The second PCR amplification was performed by
455 denaturation at 98°C for 30s; amplification for 25 cycles at 98°C for 10s, 66°C for 30s
456 and 72°C for 30s; followed by a final extension at 72°C for 2 mins. Products were
457 then purified using magnetic beads. All liquid handling was performed using a
458 Hamilton Nimbus robot equipped with a 96-head (Hamilton robotics, Kista, Sweden).
459 Samples were pooled and sequenced in a single lane on a MiSeq (300 bp paired-end,
460 Illumina Inc., San Diego, CA) at the National Genomics Infrastructure, Sweden.

461

462 *Processing of sequencing data*

463 A custom-written bioinformatics pipeline was developed in collaboration with the
464 National Bioinformatics Infrastructure Sweden to prepare .fastq files for analysis.
465 First, a custom-written script was used to de-multiplex the .fastq files by gene and
466 well. PEAR[61] was then used to merge paired-end reads, followed by removal of low-
467 quality reads using FastX[62]. The reads were then mapped to the wildtype zebrafish
468 genome (Zv11) using STAR[63]. Next, we converted files from .sam to .bam format
469 using samtools[64], after which variants - mostly indels and SNVs - were called allele

470 specifically using a custom-written variant calling algorithm in R (Danio rerio
471 Identification of Variants by Haplotype - DIVaH). A summary of all unique
472 sequences identified for the orthologues and their respective alignment report string
473 (Concise Idiosyncratic Gapped Alignment Report (CIGAR)) is shown in
474 Supplementary Table 2. All unique variants (Supplementary Table 3) located within
475 ±30bps of the CRISPR-targeted sites that were identified across the two alleles were
476 subsequently pooled, and used for functional annotation using Ensembl's VEP [65].
477 Naturally occuring variants based on sequencing of uninjected Tg*(acta2:gfp*) larvae
478 were excluded. Noteworthy, all variants per transcript get annotated individually,
479 rather than on a per transcript basis. In absence of a continuous score provided by
480 variant prediction algorithms, we attributed a score of 0.33, 0.66 and 1, and that pilot
481 experiments using *hcn4* and heart rate suggested that this was a more powerful
482 approach than not weighting.

483 Transcript-specific dosage scores were then calculated by retaining the variant with
484 the highest predicted impact on protein function, and assigning it a score of 0 (no
485 effect), 0.2 (modifier variant), 0.33 (low), 0.66 (moderate) or 1 (high). Transcript-
486 specific dosage scores were subsequently calculated by summing the allele-specific
487 scores at each embryo and target site. Since all transcripts within a target site were
488 affected virtually identically, we only used the main transcript of each target site for
489 the genetic association analysis.

490 Most larvae had successfully called sequences in all nine CRISPR-targeted sites.
491 Larvae with more than three missing sequences were excluded from the genetic
492 association analysis. For the remaining larvae, the mean dosage of the transcript was
493 imputed for missing calls. For *neo1b*, calling failed in 78 larvae (Supplementary Table
494 4). The imputed mean dosage for the main transcript of *neo1b* was still included in the

495 genetic association analysis, since the mutant allele frequency in successfully called
496 larvae was high (i.e. 0.934), and using an imputed dosage was anticipated to influence
497 the results less than to discard the gene while it had been targeted. However, the
498 results for *neo1b* should be interpreted in light of its call rate. The mutant allele
499 frequency was low for *hcn4*, *hcn4l* and *rgs6*. All three putative off-targets regions
500 (*dclk1b*, both *galnt10* orthologues, Supplementary Table 1) were classified as
501 wildtype across all larvae and had no CRISPR-Cas9 induced mutations within ±30bps
502 of the cut-site (Supplementary Table 2).

503

504 *Statistical analysis*

505 The standard deviation of NN-intervals (SDNN) and the root mean square of
506 successive differences (RMSSD) were strongly correlated at 2dpf (r^2=0.78) and 5dpf
507 (r^2=0.83), so a composite endpoint 'HRV' was calculated as the average of SDNN
508 and RMSSD. In larvae free from sinoatrial pauses and arrests, abnormal cardiac
509 morphology, impaired cardiac contractility, and edema HRV and heart rate at 2dpf
510 (n=279) or 5dpf (n=293) were inverse-normally transformed to ensure a normal
511 distribution, and to allow comparison of effect sizes across traits. Genetic effects on
512 HRV and heart rate were subsequently examined using hierarchical linear models at
513 2dpf and 5dpf separately (Stata's xtmixed), mutually adjusted for the time of imaging
514 (fixed factors), and with larvae nested in six batches (random factor with fixed slope).
515 Embryos and larvae in which a sinoatrial pause and/or arrest was observed in between
516 positioning and recording were excluded from the analysis. In a sensitivity analysis,
517 we mutually adjusted for the other outcome (i.e. heart rate and HRV).

518 In further analyses, genetic effects were examined for sinoatrial pause and arrest at
519 2dpf, as well as sinoatrial pause at 5dpf using a logistic regression analysis. Genetic
520 effects on body size were also examined, using hierarchical linear models on inverse-
521 normally transformed outcomes.

522 For dichotomous as well as continuous outcomes, genetic effects were examined
523 using an additive model, with dosage scores for all target sites as independent
524 exposures in the same model, i.e. mutually adjusted for effects of mutations in the
525 other orthologues. Additionally, larvae with two functionally knocked alleles were
526 compared with larvae free from CRISPR-induced mutations for six out of nine
527 orthologues. Missing genotypes were imputed at the mean in this analysis. For each
528 outcome, association analyses were examined for the main transcript of the
529 orthologue. *P*-values <0.05 were considered to reflect statistically significant effects.
530 All statistical analyses were performed using Stata MP 14.2.
531

Acknowledgments

The computations were performed on resources provided by SNIC through Uppsala Multidisciplinary Center for Advanced Computational Science (UPPMAX) under Project SNIC b2015283. The authors would like to acknowledge support from Science for Life Laboratory, the National Genomics Infrastructure (NGI) and UPPMAX for providing assistance in massive parallel sequencing and computational infrastructure. Support from the National Bioinformatics Infrastructure Sweden (NBIS) is also gratefully acknowledged. Constructive discussions with the Genome Engineering Zebrafish (GEZ) facility are also acknowledged.

Sources of funding

MdH is a fellow of the Swedish Heart-Lung Foundation (20170872) and is supported by project grants from the Swedish Heart-Lung Foundation (20140543, 20170678), the Swedish Research Council (2015-03657), and NIH/NIDDK (R01DK106236, R01DK107786, U01DK105554).

Disclosures

None.

551 **REFERENCES**

552 1 Thayer, J. F., Yamamoto, S. S. & Brosschot, J. F. The relationship of
553 autonomic imbalance, heart rate variability and cardiovascular disease risk
554 factors. *Int. J. Cardiol.* **141**, 122-131, (2010).
555 2 de Bruyne, M. C. *et al.* Both decreased and increased heart rate variability on
556 the standard 10-second electrocardiogram predict cardiac mortality in the
557 elderly: the Rotterdam Study. *Am. J. Epidemiol.* **150**, 1282-1288, (1999).
558 3 Dekker, J. M. *et al.* Heart rate variability from short electrocardiographic
559 recordings predicts mortality from all causes in middle-aged and elderly men -
560 The zutphen study. *Am. J. Epidemiol.* **145**, 899-908, (1997).
561 4 Nolte, I. M. *et al.* Genetic loci associated with heart rate variability and their
562 effects on cardiac disease risk. *Nature communications* **8**, 15805, (2017).
563 5 den Hoed, M. *et al.* Identification of heart rate-associated loci and their effects
564 on cardiac conduction and rhythm disorders. *Nat. Genet.* **45**, 621-631, (2013).
565 6 Nolte, I. M. *et al.* Genetic loci associated with heart rate variability and their
566 effects on cardiac disease risk. *Nature communications* **8**, 15805, (2017).
567 7 Poon, K. L. & Brand, T. The zebrafish model system in cardiovascular
568 research: A tiny fish with mighty prospects. *Glob Cardiol Sci Pract* **2013**, 9-
569 28, (2013).
570 8 Eppinga, R. N. *et al.* Identification of genomic loci associated with resting
571 heart rate and shared genetic predictors with all-cause mortality. *Nat. Genet.*
572 **48**, 1557-1563, (2016).
573 9 Arking, D. E. *et al.* Genetic association study of QT interval highlights role for
574 calcium signaling pathways in myocardial repolarization. *Nat. Genet.* **46**, 826-
575 836, (2014).
576 10 Lieschke, G. J. & Currie, P. D. Animal models of human disease: zebrafish
577 swim into view. *Nature reviews. Genetics* **8**, 353-367, (2007).
578 11 MacRae, C. A. & Peterson, R. T. Zebrafish as tools for drug discovery. *Nature*
579 *reviews. Drug discovery* **14**, 721-731, (2015).
580 12 Liu, C. C., Li, L., Lam, Y. W., Siu, C. W. & Cheng, S. H. Improvement of
581 surface ECG recording in adult zebrafish reveals that the value of this model
582 exceeds our expectation. *Sci. Rep.* **6**, 25073, (2016).
583 13 Harrington, J. K., Sorabella, R., Tercek, A., Isler, J. R. & Targoff, K. L.
584 Nkx2.5 is essential to establish normal heart rate variability in the zebrafish
585 embryo. *Am. J. Physiol. Regul. Integr. Comp. Physiol.* **313**, R265-r271,
586 (2017).
587 14 Arnaout, R. *et al.* Zebrafish model for human long QT syndrome. *Proc. Natl.*
588 *Acad. Sci. U. S. A.* **104**, 11316-11321, (2007).
589 15 Sah, R. *et al.* Ion channel-kinase TRPM7 is required for maintaining cardiac
590 automaticity. *Proc. Natl. Acad. Sci. U. S. A.* **110**, E3037-3046, (2013).
591 16 Jou, C. J. *et al.* A Functional Assay for Sick Sinus Syndrome Genetic
592 Variants. *Cell. Physiol. Biochem.* **42**, 2021-2029, (2017).
593 17 Pardo-Martin, C. *et al.* High-throughput hyperdimensional vertebrate
594 phenotyping. *Nature communications* **4**, 1467, (2013).
595 18 Early, J. J. *et al.* An automated high-resolution in vivo screen in zebrafish to
596 identify chemical regulators of myelination. *eLife* **7**, (2018).
597 19 Jarque, S. *et al.* An automated screening method for detecting compounds with
598 goitrogenic activity using transgenic zebrafish embryos. *PLoS One* **13**,
599 e0203087, (2018).

20 Howe, K. *et al.* The zebrafish reference genome sequence and its relationship to the human genome. *Nature* **496**, 498-503, (2013).
21 Varshney, G. K. *et al.* A high-throughput functional genomics workflow based on CRISPR/Cas9-mediated targeted mutagenesis in zebrafish. *Nat. Protoc.* **11**, 2357-2375, (2016).
22 Flannick, J., Johansson, S. & Njolstad, P. R. Common and rare forms of diabetes mellitus: towards a continuum of diabetes subtypes. *Nat. Rev. Endocrinol.* **12**, 394-406, (2016).
23 Ganna, A. *et al.* Quantifying the Impact of Rare and Ultra-rare Coding Variation across the Phenotypic Spectrum. *Am. J. Hum. Genet.* **102**, 1204-1211, (2018).
24 Flannick, J. A. *et al.* Genetic discovery and translational decision support from exome sequencing of 20,791 type 2 diabetes cases and 24,440 controls from five ancestries. *bioRxiv*, (2018).
25 Ramirez, J. *et al.* Thirty loci identified for heart rate response to exercise and recovery implicate autonomic nervous system. *Nature communications* **9**, 1947, (2018).
26 Kerr, K. F. *et al.* Genome-wide association study of heart rate and its variability in Hispanic/Latino cohorts. *Heart Rhythm* **14**, 1675-1684, (2017).
27 Verweij, N., van de Vegte, Y. J. & van der Harst, P. Genetic study links components of the autonomous nervous system to heart-rate profile during exercise. *Nature communications* **9**, 898, (2018).
28 Yang, J. *et al.* RGS6, a modulator of parasympathetic activation in heart. *Circ. Res.* **107**, 1345-1349, (2010).
29 Posokhova, E. *et al.* Essential role of the m2R-RGS6-IKACh pathway in controlling intrinsic heart rate variability. *PLoS One* **8**, e76973, (2013).
30 Wydeven, N., Posokhova, E., Xia, Z., Martemyanov, K. A. & Wickman, K. RGS6, but not RGS4, is the dominant regulator of G protein signaling (RGS) modulator of the parasympathetic regulation of mouse heart rate. *J. Biol. Chem.* **289**, 2440-2449, (2014).
31 Ellinor, P. T. *et al.* Meta-analysis identifies six new susceptibility loci for atrial fibrillation. *Nat. Genet.* **44**, 670-675, (2012).
32 Shi, W. *et al.* Distribution and prevalence of hyperpolarization-activated cation channel (HCN) mRNA expression in cardiac tissues. *Circ. Res.* **85**, e1-6, (1999).
33 Ludwig, A. *et al.* Two pacemaker channels from human heart with profoundly different activation kinetics. *EMBO J.* **18**, 2323-2329, (1999).
34 Stieber, J. *et al.* The hyperpolarization-activated channel HCN4 is required for the generation of pacemaker action potentials in the embryonic heart. *Proc. Natl. Acad. Sci. U. S. A.* **100**, 15235-15240, (2003).
35 Bucchi, A. *et al.* Identification of the molecular site of ivabradine binding to HCN4 channels. *PLoS One* **8**, e53132, (2013).
36 Swedberg, K. *et al.* Ivabradine and outcomes in chronic heart failure (SHIFT): a randomised placebo-controlled study. *Lancet* **376**, 875-885, (2010).
37 Burggren, W. W. & Pinder, A. W. Ontogeny of cardiovascular and respiratory physiology in lower vertebrates. *Annu. Rev. Physiol.* **53**, 107-135, (1991).
38 Rossi, A. *et al.* Genetic compensation induced by deleterious mutations but not gene knockdowns. *Nature* **524**, 230-233, (2015).
39 El-Gebali, S. *et al.* The Pfam protein families database in 2019. *Nucleic Acids Res.* **47**, D427-d432, (2019).

650 40 Baruscotti, M. *et al.* A gain-of-function mutation in the cardiac pacemaker
651 HCN4 channel increasing cAMP sensitivity is associated with familial
652 Inappropriate Sinus Tachycardia. *Eur. Heart J.* **38**, 280-288, (2017).
653 41 Kozasa, Y. *et al.* HCN4 pacemaker channels attenuate the parasympathetic
654 response and stabilize the spontaneous firing of the sinoatrial node. *J. Physiol.*
655 **596**, 809-825, (2018).
656 42 Battle, A., Brown, C. D., Engelhardt, B. E. & Montgomery, S. B. Genetic
657 effects on gene expression across human tissues. *Nature* **550**, 204-213, (2017).
658 43 Sudhof, T. C. Synaptotagmins: why so many? *J. Biol. Chem.* **277**, 7629-7632,
659 (2002).
660 44 Chapman, E. R. How does synaptotagmin trigger neurotransmitter release?
661 *Annu. Rev. Biochem.* **77**, 615-641, (2008).
662 45 Wu, R. S. *et al.* A Rapid Method for Directed Gene Knockout for Screening in
663 G0 Zebrafish. *Dev. Cell* **46**, 112-125.e114, (2018).
664 46 Newton-Cheh, C. *et al.* Genome-wide association study of
665 electrocardiographic and heart rate variability traits: the Framingham Heart
666 Study. *BMC Med. Genet.* **8 Suppl 1**, S7, (2007).
667 47 Dong, C. *et al.* Genetic variants in LEKR1 and GALNT10 modulate sex-
668 difference in carotid intima-media thickness: a genome-wide interaction study.
669 *Atherosclerosis* **240**, 462-467, (2015).
670 48 Locke, A. E. *et al.* Genetic studies of body mass index yield new insights for
671 obesity biology. *Nature* **518**, 197-206, (2015).
672 49 Justice, A. E. *et al.* Genome-wide meta-analysis of 241,258 adults accounting
673 for smoking behaviour identifies novel loci for obesity traits. *Nature*
674 *communications* **8**, 14977, (2017).
675 50 Ng, M. C. Y. *et al.* Discovery and fine-mapping of adiposity loci using high
676 density imputation of genome-wide association studies in individuals of
677 African ancestry: African Ancestry Anthropometry Genetics Consortium.
678 *PLoS genetics* **13**, e1006719, (2017).
679 51 Varshney, G. K. *et al.* High-throughput gene targeting and phenotyping in
680 zebrafish using CRISPR/Cas9. *Genome Res.* **25**, 1030-1042, (2015).
681 52 Louis, A., Nguyen, N. T., Muffato, M. & Roest Crollius, H. Genomicus
682 update 2015: KaryoView and MatrixView provide a genome-wide perspective
683 to multispecies comparative genomics. *Nucleic Acids Res.* **43**, D682-689,
684 (2015).
685 53 Labun, K., Montague, T. G., Gagnon, J. A., Thyme, S. B. & Valen, E.
686 CHOPCHOP v2: a web tool for the next generation of CRISPR genome
687 engineering. *Nucleic Acids Res.* **44**, W272-276, (2016).
688 54 Moreno-Mateos, M. A. *et al.* CRISPRscan: designing highly efficient sgRNAs
689 for CRISPR-Cas9 targeting in vivo. *Nature methods* **12**, 982-988, (2015).
690 55 Jao, L. E., Wente, S. R. & Chen, W. Efficient multiplex biallelic zebrafish
691 genome editing using a CRISPR nuclease system. *Proc. Natl. Acad. Sci. U. S.*
692 *A.* **110**, 13904-13909, (2013).
693 56 Whitesell, T. R. *et al.* An alpha-smooth muscle actin (acta2/alphasma)
694 zebrafish transgenic line marking vascular mural cells and visceral smooth
695 muscle cells. *PLoS One* **9**, e90590, (2014).
696 57 Hou, J. H., Kralj, J. M., Douglass, A. D., Engert, F. & Cohen, A. E.
697 Simultaneous mapping of membrane voltage and calcium in zebrafish heart in
698 vivo reveals chamber-specific developmental transitions in ionic currents.
699 *Front. Physiol.* **5**, 344, (2014).

58 Niazi, M. K. K., Nilsson, M. F., Danielsson, B. R. & Bengtsson, E. Fully Automatic Heart Beat Rate Determination in Digital Video Recordings of Rat Embryos. (2009).
59 Lamprecht, M. R., Sabatini, D. M. & Carpenter, A. E. CellProfiler: free, versatile software for automated biological image analysis. *Biotechniques* **42**, 71-75, (2007).
60 Koressaar, T. & Remm, M. Enhancements and modifications of primer design program Primer3. *Bioinformatics* **23**, 1289-1291, (2007).
61 Zhang, J., Kobert, K., Flouri, T. & Stamatakis, A. PEAR: a fast and accurate Illumina Paired-End reAd mergeR. *Bioinformatics* **30**, 614-620, (2014).
62 Pearson, W. R., Wood, T., Zhang, Z. & Miller, W. Comparison of DNA sequences with protein sequences. *Genomics* **46**, 24-36, (1997).
63 Dobin, A. *et al.* STAR: ultrafast universal RNA-seq aligner. *Bioinformatics* **29**, 15-21, (2013).
64 Li, H. *et al.* The Sequence Alignment/Map format and SAMtools. *Bioinformatics* **25**, 2078-2079, (2009).
65 McLaren, W. *et al.* The Ensembl Variant Effect Predictor. *Genome Biol.* **17**, 122, (2016).

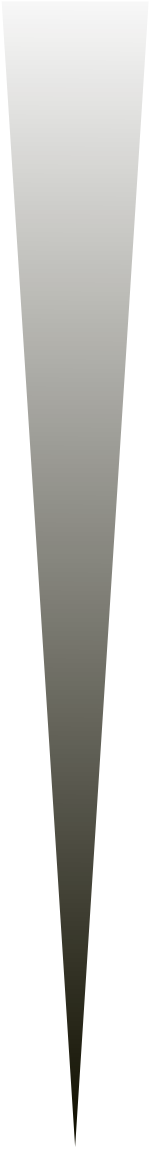

Figure 1: Experimental pipeline describing the workflow from candidate gene selection to trait association. dpf = days post fertilization. VEP = Variant Effect Predictor.
1: Nolte et al. 2017

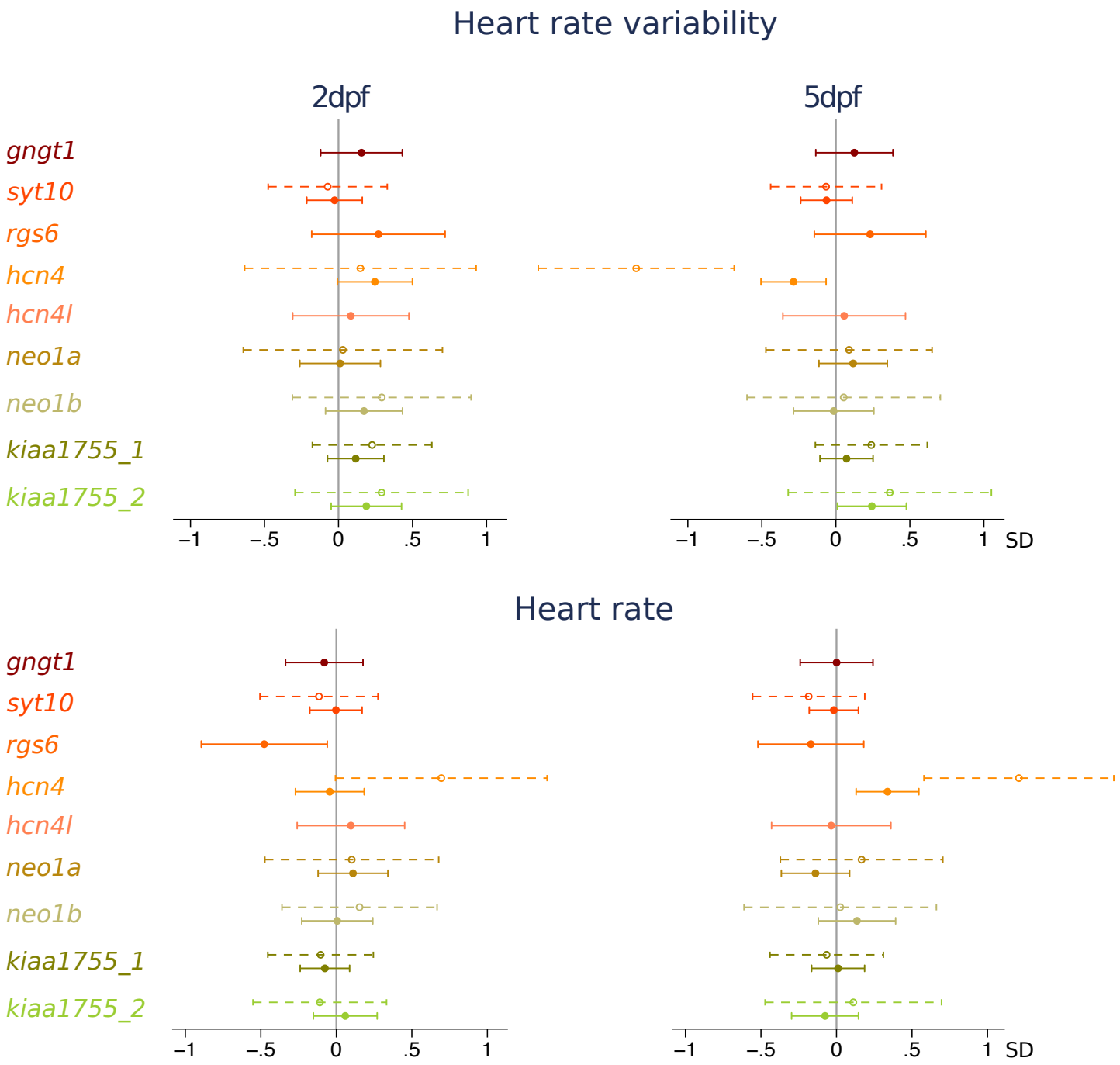

Figure 2: Effect of mutations in candidate genes on heart rhythm and rate at 2 (n=234) and 5dpf (n=285). Dots and whiskers show the effect size and its 95% confidence interval for each additional mutated allele (solid line), weighted by its predicted effect on protein function. Dotted bars indicate the results of comparing larvae with two functionally knocked alleles with wildtype larvae. Effects were adjusted for the number of mutated alleles in the other genes, as well as time of day (fixed factor), with larvae nested in batches (random factor).

Table 1: Selected candidate genes and their zebrafish orthologues in GWAS-identified heart rate variability associated loci

rsID	Chr	Human gene	ENSG	Zebrafish orthologue	ENSDARG
rs4262, rs180238	7	*GNG11*	ENSG00000127920	*gngt1*	ENSDARG00000035798
rs7980799, rs1351682, rs1384598	12	*SYT10*	ENSG00000110975	*syt10*	ENSDARG00000045750
rs4899412, rs2052015, rs2529471, rs36423	14	*RGS6*	ENSG00000182732	*rgs6*	ENSDARG00000015627
rs2680344	15	*HCN4*	ENSG00000138622	*hcn4*	ENSDARG00000061685
				hcn4l	ENSDARG00000074419
rs1812835	15	*NEO1*	ENSG00000067141	*neo1a*	ENSDARG00000102855
				neo1b	ENSDARG00000075100
rs6123471	20	*KIAA1755*	ENSG00000149633	*quo*	ENSDARG00000073684
				si:dkey-65j6.2	ENSDARG00000103586

rsID refers to the lead SNP(s) of the GWAS-identified loci (Nolte et. al, 2017). Multiple independent SNPs per locus can be present.

Table 2: Effects of mutations in *hcn4* on sinoatrial pauses and arrests at 2dpf

Age	Gene	Outcome	n total	n cases	OR	LCI	UCI	P
2	*hcn4*	SA arrest	248	36	2.644	1.402	4.986	2.66E-03
		SA pause	297	39	2.749	1.461	5.171	1.71E-03

Associations of sinoatrial pauses and arrests with the number of mutated alleles in *hcn4*, weighted by their predicted effect on protein function. Associations were analyzed using logistic regression, and were adjusted for time of day and for the weighted number of mutated alleles in the other genes as fixed factors.

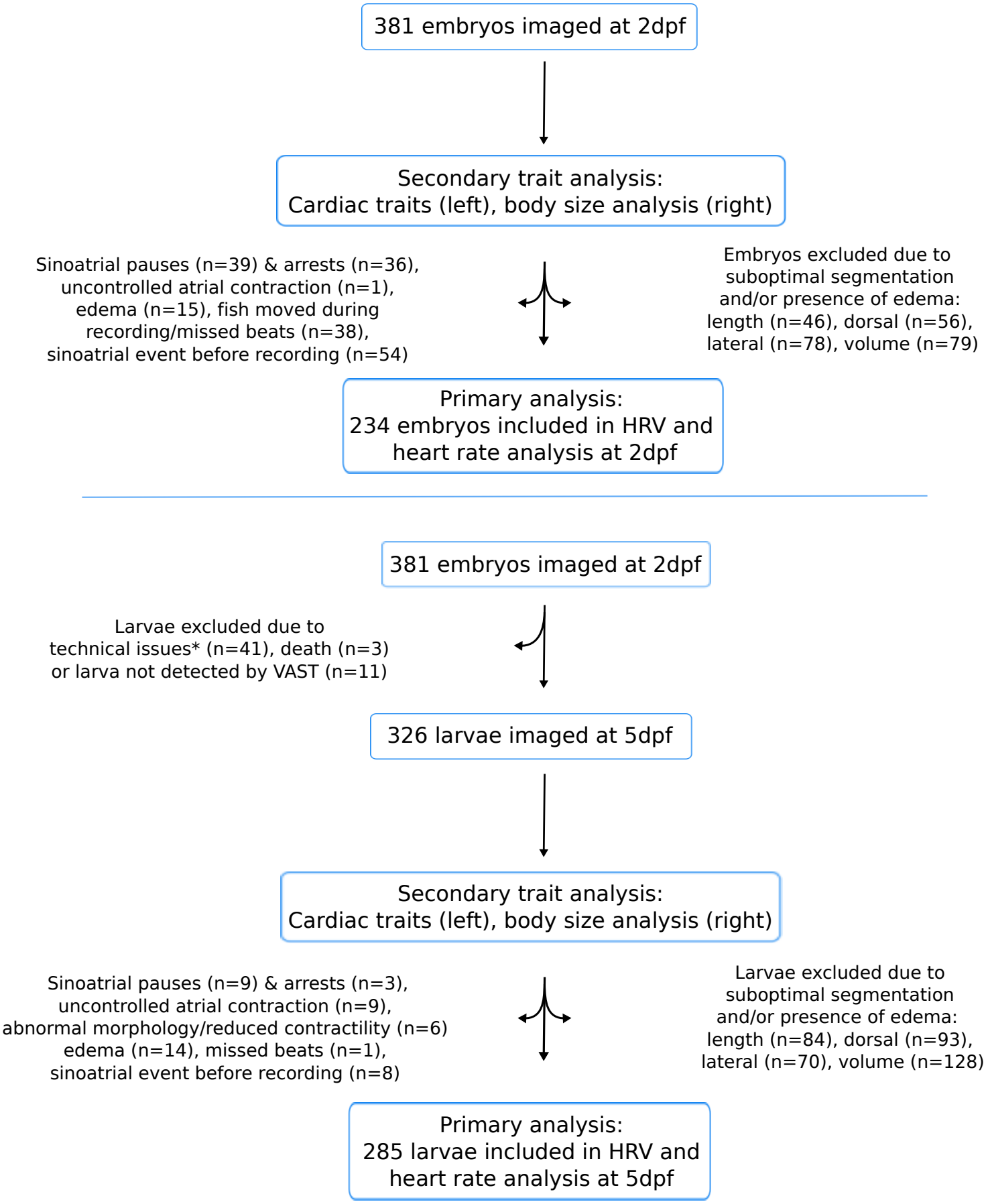

Supplementary Figure 1: Flow chart showing the number of included larvae in the analysis and reasons for exclusions. Embryos/larvae can show more than one phenotype. *Technical issues refers to not being able to image due to microscope complications. VAST: Vertebrate automated screening technology.

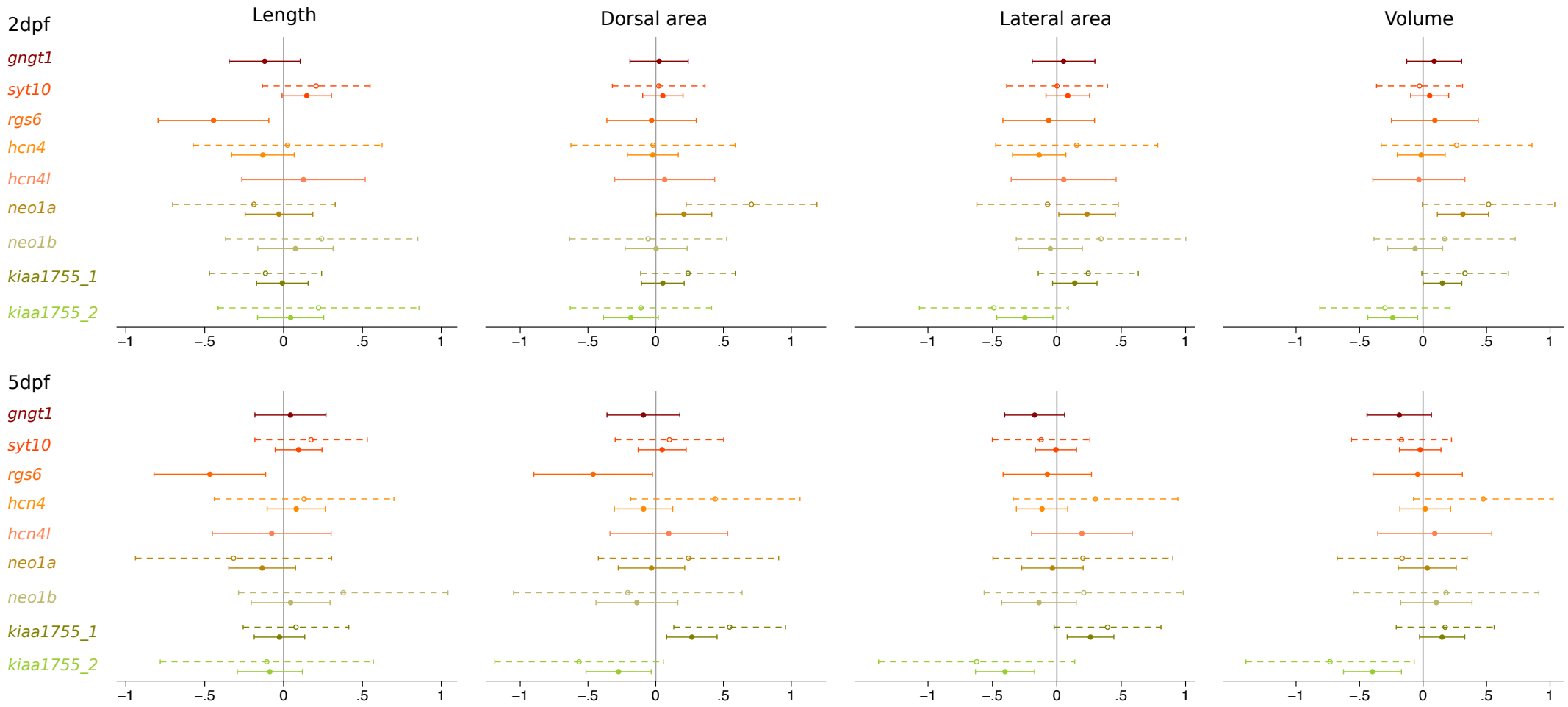

Supplementary Figure 2: Effect of mutations in candidate genes on length, dorsal and lateral area, and volume at 2 (upper part) and 5dpf (lower part). Dots and whiskers show the effect size and its 95% confidence interval for each additional mutated allele (solid line), weighted by its predicted effect on protein function. Dotted bars indicate the results of comparing larvae with two functionally knocked alleles with wildtype larvae. Effects were adjusted for the number of mutated alleles in the other genes, as well as time of day (fixed factor), with larvae nested in batches (random factor).

Supplementary Table 1: Overview of zebrafish orthologues and designed gRNAs

Zebrafish orthologue	ENSDARG	Conservation Zebrafish - Human	Conservation Zebrafish - Spotted gar	Main transcript	Target sequence gRNA	Exon target (transcript name)	CRISPR-scan rank	ChopChop rank	Activity test rank	Predicted off-targets	Nr of mismat-ches	Genomic location of potential off-target 1	ENSDARG (gene-ID) of potential off-target 1, Feature	ENSG (gene-ID) of potential off-target 1	Genomic location of potential off-target 2	ENSDARG (gene-ID) of potential off-target 2, Feature	ENSG (gene-ID) of potential off-target 2	Primer forward	Primer reverse	Amplicon size
gngt1	ENSDARG00000035798	17	21	ENSDART00000051950	gGACCTGGATAAGGCGAAGA	2/3 (gngt1-001); 1/2 (gngt1-002)	62	4/13 (yellow)	moderate	1	3	chr25:17488676	ENSDARG00000051959 (*zgc:66449*), intron (3/6), intron (4/4)	no human orthologue				GTCCATTTTCCAGAGTGGAGAC	gCCCATAACACAATTGCTTACC	207
syt10	ENSDARG00000045750	0	1	ENSDART00000136049	GGCTGATGCCGTCCTCTGTG	1/7 (syt10-001); 1/7 (syt10-201)	36	6/129 (green)	low	0								TAGGATATGGACTTGGACGCAT	TTACCTGGTATGTTGCTCTCCA	227
rgs6	ENSDARG00000015627	9	20	ENSDART00000135513	GGCCTCTCAGGACCAAGG	1/17 (rgs6-201); 2/18 (rgs6-001)	62	1/107 (green)	low	0								AAGGCTAATTCATTGTCTGGGA	GCATGTCAAATGTAAAGGCAAA	169
hcn4	ENSDARG00000061685	6	3	ENSDART00000136140	GGAGAGCCCTCCTGGAGCCG	1/8 (hcn4-001)	59	11/280 (green)	high	2	3/3	chr21:45844184	ENSDARG00000103825 (*galnt10*), exon (1/3)	ENSG00000164574 (GALNT10)	chrUn_KN150614v1:3424	ENSDARG00000100453 (*galnt10*), exon (6/8)	ENSG00000164574 (GALNT10)	CCTTTCGTCCATCACCAGTC	CCGCTTGATAATACCTCTCGTC	230
hcn4l	ENSDARG00000074419	3	3	ENSDART00000088249	gGCCTGGATAGTGTTTAACG	2/8 (hcn4l-201); 1/7 (hcn4l-001)	/	2/191 (green)	low	0								TTACTGGGACCTGATCATGCTT	AAGATGTAATCCACAGGGATGG	235
neo1a	ENSDARG00000102855	1	5	ENSDART00000158160	GGAGCCGTCGGATACACTAG	1/4 (neo1a-001); 2/29 (neo1a-201); 2/30 (neo1a-202)	48	2/55 (green)	very high	0								TTCTGTGTCTCCACAGGATCAG	CCTCATCGGGTTTATTGTGTTT	215
neo1b	ENSDARG00000075100	2	6	ENSDART00000115280	GGACAGAGATGCTCGGCCTG	3/29 (neo1b-201)	58	18/354 (green)	very high	0								CAGCTCTCTCTCTCATTGGCTT	TATGGTGCAACGGTAGAGTCC	206
quo	ENSDARG00000073684	2	5	ENSDART00000109679	GGAGATCCGGTTGCCCTGTG	2/22 (quo-001); 3/23 (quo-201)	83	12/331 (green)	very high	0								ATGACCGTAAGTCAAGGGAAAA	TGAATCTTGTCTAATGGCGTTG	153
si:dkey-65j6.2	ENSDARG00000103586	3	5	ENSDART00000158832	GGACGGTTTGGCTCCAGCAG	1/23 (si:dkey-65j6.2-201); 3/25 (si:dkey-65j6.2-001)	59	14/303 (green)	very high	2	3/3	chr15:32969618	ENSDARG00000104664 (*dclk1b*), exon (3/16), exon (4/17)	ENSG00000133083 (DCLK1)	chr22:28819880	ENSDARG00000071083 (*si:dkeyp-34c12.1*), Intron (7/7), Exon (8/9)	no human orthologue	AGCCATTACACCCAAAGAAAAA	GGGAATCATTTCGAAGTAGCTG	152

Table showing zebrafish genes, main transcript used for the analysis and gRNAs; rsID refers to the lead SNP(s) of the GWAS-identified loci (Nolte et. al, 2017), multiple independent SNPs per locus can be present; For simplicity, *quo* is referred to as *kiaa1755_1*, and *si:dkey-65j6.2* as *kiaa1755_2*; Conservation refers to the number of genes that are preserved in the same locus across species according to Genomicus; A small "g" in the gRNA target sequence indicates a manually introduced nucleotide change to guanine; Exon target lists the targeted transcripts and their respective exons; ChopChop rank indicates the rank of the gRNA chosen by ChopChop and its rating (green being a "good"-predicted target, yellow an average target, details can be found on the ChopChop homepage; Activity test rank quantification: Low: 8 of 8 larvae showed wildtype sequence and fewer than 4 of 8 also contained an indel sequence, Moderate: 8 of 8 larvae showed the wildtype sequence and >4 of 8 also contained an indel sequence, High: 8 of 8 larvae showed wildtype as well as indel sequences, Very high: Fewer than 4 of 8 larvae showed wildtype sequence and all larvae showed indels; ENSDARG of potential off-target refers to the ENSEMBL gene-ID of the potential off-target and where the potential target is located (Feature), zgc:66449 and si:dkeyp-34c12.1 have no human orthologue, whereas galnt10 and dckl1b may exert an effect on heart rate and/or rhythm.

Supplementary Table 2: Unique Cigars

Orthologue	Sequence	Cigar	Mean Nr reads	Nr alleles	SD reads
	CTCATCGTAAGCAGCAGTAAGTTTGCTTATTTCCAGTATATTGAACATCAAATATAATCCATTCATTCAACACAACAT GTAAATGATGTGATTGTTTGATTTCATGCAGAAAATGCCGATCATAGATGTAGAAAATATGACTGACCTGGATAAG GCGAAGATGGAAGTAACCCAGCTCAAAACTGAGGTGAAGCTAGAAAGGGCGAA	45M1S41M1S119M	498	336	381
	CTCATCGTAAGCAGCAGTAAGTTTGCTTATTTCCAGTATATTGAATATCAAATATAATCCATTCATTCAACACAACAT GTAAATGATATGATTGTTTGATTTCATGCAGAAAATGCCGATCATAGATGTAGAAAATATGACTGACCTGGATAAG GCGAAGATGGAAGTAACCCAGCTCAAAACTGAGGTGAAGCTAGAAAGGGCGAA	207M	517	267	372
	CTCATCGTAAGCAGCAGTAAGTTTGCTTATTTCCAGTATATTGAACATCAAATATAATCCATTCATTCAACACAACAT GTAAATGATGTGATTGTTTGATTTCATGCAGAAAATGCCGATCATAGATGTAGAAAATATGACTGACCTGGATAAG GCGTTTTGGAAGTAACCCAGCTCAAAACTGAGGTGAAGCTAGAAAGGGCGAA	45M1S41M1S69M1D3S46M	544	69	405
	CTCATCGTAAGCAGCAGTAAGTTTGCTTATTTCCAGTATATTGAATATCAAATATAATCCATTCATTCAACACAACAT GTAAATGATATGATTGTTTGATTTCATGCAGAAAATGCCGATCATAGATGTAGAAAATATGACTGACCTGGATAAG ATGGAAGTAACCCAGCTCAAAACTGAGGTGAAGCTAGAAAGGGCGAA	151M6D50M	500	63	364
	CTCATCGTAAGCAGCAGTAAGTTTGCTTATTTCCAGTATATTGAACATCAAATATAATCCATTCATTCAACACAACAT GTAAATGATGTGATTGTTTGATTTCATGCAGAAAATGCCGATCATAGATGTAGAAAATATGACTGACCTGGATAAG ATGGAAGTAACCCAGCTCAAAACTGAGGTGAAGCTAGAAAGGGCGAA	45M1S41M1S63M6D50M	584	13	479
gngt1	CTCATCGTAAGCAGCAGTAAGTTTGCTTATTTCCAGTATATTGAATATCAAATATAATCCATTCATTCAACACAACAT GTAAATGATATGATTGTTTGATTTCATGCAGAAAATGCCGATCATAGATGTAGAAAATATGACTGACCTGGATAAG GCGATGATGGAAGTAACCCAGCTCAAAACTGAGGTGAAGCTAGAAAGGGCGAA	158M1S48M	504	4	221
	CTCATCGTAAGCAGCAGTAAGTTTGCTTATTTCCAGTATATTGAACATCAAATATAATCCATTCATTCAACACAACAT GTAAATGATGTGATTGTTTGATTTCATGCAGAAAATGCCGATCATAGATGTAGAAAATATGACTGACCTGGATAAG GCGATGGAAGTAACCCAGCTCAAAACTGAGGTGAAGCTAGAAAGGGCGAA	45M1S41M1S68M3D48M	606	3	119
	CTCATCGTAAGCAGCAGTAAGTTTGCTTATTTCCAGTATATTGAACATCAAATATAATCCATTCATTCAACACAACAT GTAAATGATGTGATTGTTTGATTTCATGCAGAAAATGCCGATCATAGATGTAGAAAATATGACTGACCTGGATAAG GCGAAGTAACCCAGAAGTAACCCAGCTCAAAACTGAGGTGAAGCTAGAAAGGGCGAA	45M1S41M1S72M4I3S44M	526	2	143
	CTCATCGTAAGCAGCAGTAAGTTTGCTTATTTCCAGTATATTGAACATCAAATATAATCCATTCATTCAACACAACAT GTAAATGATGTGATTGTTTGATTTCATGCAGAAAATGCCGATAATAGATGTAGAAAATATGACTGACCTGGATAAG GCGTTTTGGAAGTAACCCAGCTCAAAACTGAGGTGAAGCTAGAAAGGGCGAA	45M1S41M1S32M1S36M1D3S46M	48	1	-
	ATCATCGTAAGCAGCAGTAAGTTTGCTTATTTCCAGTATATTGAACATCAAATATAATCCATTCATTCAACACAACAT GTAAATGATGTGATTGTTTGATTTCATGCAGAAAATGCCGATCATAGATGTAGAAAATATGACTGACCTGGATAAG GCGTTTTGGAAGTAACCCAGCTCAAAACTGAGGTGAAGCTAGAAAGGGCGAA	1S44M1S41M1S69M1D3S46M	10	1	-
	CTCATCGTAAGCAGCAGTAAGTTTGCTTATTTCCAGTATATTGAATATCAAATATAATCCATTCATTCAACACAACAT GTAAATGATGTGATTGTTTGATTTCATGCAGAAAATGCCGATCATAGATGTAGAAAATATGACTGACCTGGATAAG GCGAAGATGGAAGTAACCCAGCTCAAAACTGAGGTGAAGCTAGAAAGGGCGAA	87M1S119M	3	1	-
	CGGTCTCTCTCCATTCCCGTACGCATCAGCTGCACTCAGCAGCTCACATGGTGCCCCAATGAACTCTCGCCCTCACG CATCGTCCAACATACAATGGATTAACAGGAAAGACATGAATGTCCGCACAGAGGACGGCATCAGCCTGTGCCAAA GGGCTCTCCAAATAGTGACAGAGCTGTGCCTCGCCGGGCACGTCGACCGGGAGAAATGCGCGGATATATTTCCAC	227M	1024	518	644
syt10	CGGTCTCTCTCCATTCCCGTACGCATCAGCTGCACTCAGCAGCTCACATGGTGCCCCAATGAACTCTCGCCCTCACG CATCGTCCAACATACAATGGATTAACAGGAAAGACATGAATGTCCGCACAAGAGGACGGCATCAGCCTGTGCCAA AGGGCTCTCCAAATAGTGACAGAGCTGTGCCTCGCCGGGCACGTCGACCGGGAGAAATGCGCGGATATATTTCCA C	126M1I101M	735	46	462
	CGGTCTCTCTCCATTCCCGTACGCATCAGCTGCACTCAGCAGCTCACATGGTGCCCCAATGAACTCTCGCCCTCACG CATCGTCCAACATACAATGGATTAACAGGAAAGACATGAATGTCCGACGGCATCAGCCTGTGCCAAAGGGCTCTC CAAATAGTGACAGAGCTGTGCCTCGCCGGGCACGTCGACCGGGAGAAATGCGCGGATATATTTCCAC	122M8D97M	606	45	397

Continued Supplementary Table 2

Orthologue	Sequence	Cigar	Mean Nr reads	Nr alleles	SD reads
	CGGTCTCTCTCCATTCCCGTACGCATCAGCTGCACTCAGCAGCTCACATGGTGCCCCAATGAACTCTCGCCCTCACG CATCGTCCAACATACAATGGATTAACAGGAAAGACATGAATGTACAGCTGATGCGTACGGGAATGGAGAGGACG GCATCAGCCTGTGCCAAAGGGCTCTCCAAATAGTGACAGAGCTGTGCCTCGCCGGGCACGTCGACCGGGAGAAAT GCGCGGATATATTTCCAC	120M1S9I2M1S2M8I101M	793	43	405
	CGGTCTCTCTCCATTCCCGTACGCATCAGCTGCACTCAGCAGCTCACATGGTGCCCCAATGAACTCTCGCCCTCACG CATCGTCCAACATACAATGGATTAACAGGAAAGACATGAATGTCCGCACATGGACGGCATCAGCCTGTGCCAAAG GGCTCTCCAAATAGTGACAGAGCTGTGCCTCGCCGGGCACGTCGACCGGGAGAAATGCGCGGATATATTTCCAC	127M1S1D98M	368	42	246
	CGGTCTCTCTCCATTCCCGTACGCATCAGCTGCACTCAGCAGCTCACATGGTGCCCCAATGAACTCTCGCCCTCACG CATCGTCCAACATACAATGGATTAACAGGAAAGACGGCATCAGCCTGTGCCAAAGGGCTCTCCAAATAGTGACAG AGCTGTGCCTCGCCGGGCACGTCGACCGGGAGAAATGCGCGGATATATTTCCAC	109M21D97M	667	19	267
syt10	CGGTCTCTCTCCATTCCCGTACGCATCAGCTGCACTCAGCAGCTCACATGGTGCCCCAATGAACTCTCGCCCTCACG CATCGTCCAACATACAATGGATTAACAGGAAAGACATGAATGTCCGGACGGCATCAGCCTGTGCCAAAGGGCTCT CCAAATAGTGACAGAGCTGTGCCTCGCCGGGCACGTCGACCGGGAGAAATGCGCGGATATATTTCCAC	122M7D98M	963	16	431
	CGGTCTCTCTCCATTCCCGTACGCATCAGCTGCACTCAGCAGCTCACATGGTGCCCCAATGAACTCTCGCCCTCACG CATCGTCCAACATACAATGGATTAACAGGAAAGACATGAATGTCCGCACGGCATCAGACGGCATCAGCCTGTGCC AAAGGGCTCTCCAAATAGTGACAGAGCTGTGCCTCGCCGGGCACGTCGACCGGGAGAAATGCGCGGATATATTTC CAC	126M1S1M3I2S97M	937	11	645
	CGGTCTCTCTCCATTCCCGTACGCATCAGCTGCACTCAGCAGCTCACATGGTGCCCCAATGAACTCTCGCCCTCACG CATCGTCCAACATACAATGGATTAACAGGAAAGACATGAATGTCCGCACGGCATCAGCCTGTGCCAAAGGGCTCT CCAAATAGTGACAGAGCTGTGCCTCGCCGGGCACGTCGACCGGGAGAAATGCGCGGATATATTTCCAC	124M7D96M	502	11	300
	CGGTCTCTCTCCATTCCCGTACGCATCAGCTGCACTCAGCAGCTCACATGGTGCCCCAATGAACTCTCGCCCTCACG CATCGTCCAACATACAATGGATTAACAGGAAAGACATGAATGTCCGCCTGTCAGCCTGTGCCAAAGGGCTCTCCAA ATAGTGACAGAGCTGTGCCTCGCCGGGCACGTCGACCGGGAGAAATGCGCGGATATATTTCCAC	124M1S10D2S90M	524	4	229
	CGGTCTCTCTCCATTCCCGTACGCATCAGCTGCACTCAGCAGCTCACATGGTGCCCCAATGAACTCTCGCCCTCACG CATCGTCCAACATACAATGGATTAACAGGAAAGACATGAATGTCCGAGGACGGCATCAGCCTGTGCCAAAGGGCT CTCCAAATAGTGACAGAGCTGTGCCTCGCCGGGCACGTCGACCGGGAGAAATGCGCGGATATATTTCCAC	122M5D100M	1247	3	670
	GTGACAGTACCTTCCTGTATGCAATCATGTTGGGTGAGTCCTCATCTGGGTCGGCTATGCCCACCGCACCTTGGTCC TGAGAGGCCTGAGCCATGCTTGATTGCTGGGTCTCTCTTTCTGTGTCTGTGGGGAACGGGCACAACAGAAAAGGA ATGAGTCCCAGAACAGG	169M	1431	728	813
	GTGACAGTACCTTCCTGTATGCAATCATGTTGGGTGAGTCCTCATCTGGGTCGGCTATGCCCACCGCACTTGGTCCT GAGAGGCCTGAGCCATGCTTGATTGCTGGGTCTCTCTTTCTGTGTCTGTGGGGAACGGGCACAACAGAAAAGGAA TGAGTCCCAGAACAGG	68M1D100M	784	24	453
rgs6	GTGACAGTACCTTCCTGTATGCAATCATGTTGGGTGAGTCCTCATCTGGGTCGGCTATGCCCACCGCATTGGTCCT GAGAGGCCTGAGCCATGCTTGATTGCTGGGTCTCTCTTTCTGTGTCTGTGGGGAACGGGCACAACAGAAAAGGAA TGAGTCCCAGAACAGG	68M2D99M	540	7	195
	GTGACAGTACCTTCCTGTATGCAATCATGTTGGGTGAGTCCTCATCTGGGTCGGCTATGCCCACCGCATAGTCCTG AGAGGCCTGAGCCATGCTGAGCCATGCTTGATTGCTGGGTCTCTCTTTCTGTGTCTGTGGGGAACGGGCACAACA GAAAAGGAATGAGTCCCAGAACAGG	68M3D1M1S12M10I84M	920	4	287
	GTGACAGTACCTTCCTGTATGCAATCATGTTGGGTGAGTCCTCATCTGGGTCGGCTATGTGGTCCTGAGAGGCCTG AGCCATGCTTGATTGCTGGGTCTCTCTTTCTGTGTCTGTGGGGAACGGGCACAACAGAAAAGGAATGAGTCCCAG AACAGG	59M12D98M	1424	1	-
hcn4	GTCCGGCAGTATCTGCTCGATGCCTTCCAGCTTAATAAAGCCAGCCTGCTGATCCGGGATGCCCTGATGCTGGCTC GAACCGGCGGCTTCCTCTCCGCCTCCCCCGCCGCTCTGCGCACCGGGCTCCGCGCCGCCACCCGCGGCTCCAGGAG GGCTCTCCTCGCTAGGAGTGACCTCTCCGTCCGTGATCAGACGCCTTTCCTCGGCTACATCCGAGTCGTGGACGTG CC	230M	1380	638	789

Continued Supplementary Table 2

Orthologue	Sequence	Cigar	Mean Nr reads	Nr alleles	SD reads
	GTCCGGCAGTATCTGCTCGATGCCTTCCAGCTTAATAAAGCCAGCCTGCTGATCCGGGATGCCCTGATGCTGGCTCGAACCGGCGGCTTCCTCTCCGCCTCCCCCGCCGCTCTGCGCACCGGGCTCCGCGCCGCCACCCGCGCCGCCACCCAGGAGGGCTCTCCTCGCTAGGAGTGACCTCTCCGTCCGTGATCAGACGCCTTTCCTCGGCTACATCCGAGTCGTGGACGTGCC	142M1S1M4I1S85M	725	48	343
	GTCCGGCAGTATCTGCTCGATGCCTTCCAGCTTAATAAAGCCAGCCTGCTGATCCGGGATGCCCTGATGCTGGCTCGAACCGGCGGCTTCCTCTCCGCCTCCCCCGCCGCTCTGCGCACCGGGCTCCGCGCCGCCATCCGCGCCGCCACCCTCCAGGAGGGCTCTCCTCGCTAGGAGTGACCTCTCCGTCCGTGATCAGACGCCTTTCCTCGGCTACATCCGAGTCGTGGACGTGCC	136M1S5M7I1S87M	1314	16	225
	GTCCGGCAGTATCTGCTCGATGCCTTCCAGCTTAATAAAGCCAGCCTGCTGATCCGGGATGCCCTGATGCTGGCTCGAACCGGCGGCTTCCTCTCCGCCTCCCCCGCCGCTCTGCGCACCGGGCTCCGCGCCGCCACCCGCGGCTCTCCTCCAGGAGCTCCAGGGCTCTCCTCGCTAGGAGTGACCTCTCCGTCCGTGATCAGACGCCTTTCCTCGGCTACATCCGAGTCGTGGACGTGCC	143M5I7M6I80M	799	15	383
	GTCCGGCAGTATCTGCTCGATGCCTTCCAGCTTAATAAAGCCAGCCTGCTGATCCGGGATGCCCTGATGCTGGCTCGAACCGGCGGCTTCCTCTCCGCCTCCCCCGCCGCTCTGCGCACCGGGCTCCGCGCCGCCCTCCAGGAGGGCTCTCCTCGCTAGGAGTGACCTCTCCGTCCGTGATCAGACGCCTTTCCTCGGCTACATCCGAGTCGTGGACGTGCC	135M8D87M	917	13	563
hcn4	GTCCGGCAGTATCTGCTCGATGCCTTCCAGCTTAATAAAGCCAGCCTGCTGATCCGGGATGCCCTGATGCTGGCTCGAACCGGCGGCTTCCTCTCCGCCTCCCCCGCCGCTCTGCGCACCGGGCTCCGCGCCGCCACCCGCCCTCCAGGAGGGCTCTCCTCGCTAGGAGTGACCTCTCCGTCCGTGATCAGACGCCTTTCCTCGGCTACATCCGAGTCGTGGACGTGCC	141M1D1S87M	987	11	377
	GTCCGGCAGTATCTGCTCGATGCCTTCCAGCTTAATAAAGCCAGCCTGCTGATCCGGGATGCCCTGATGCTGGCTCGAACCGGCGGCTTCCTCTCCGCCTCCCCCGCCGCTCTGCGCACCGGGCTCCGCGCCGCCACCCACCCAGGAGGGCTCTCCTCGCTAGGAGTGACCTCTCCGTCCGTGATCAGACGCCTTTCCTCGGCTACATCCGAGTCGTGGACGTGCC	139M1S1M4D85M	1302	10	587
	GTCCGGCAGTATCTGCTCGATGCCTTCCAGCTTAATAAAGCCAGCCTGCTGATCCGGGATGCCCTGATGCTGGCTCGAACCGGCGGCTTCCTCTCCGCCTCCCCCGCCGCTCTGCGCACCGGGCTCCGCGCCGCCACCCGCGGGCCCTCCAGGAGGGCTCTCCTCGCTAGGAGTGACCTCTCCGTCCGTGATCAGACGCCTTTCCTCGGCTACATCCGAGTCGTGGACGTGCC	143M3I87M	694	2	49
	GTCCGGCAGTATCTGCTCGATGCCTTCCAGCTTAATAAAGCCAGCCTGCTGATCCGGGATGCCCTGATGCTGGCTCGAACCGGCGGCTTCCTCTCCGCCTCCCCCGCCGCTCTGCGCACCGGGCTCCGCGCCGCCACCCGCATCCAGGAGGGCTCTCCTCGCTAGGAGTGACCTCTCCGTCCGTGATCAGACGCCTTTCCTCGGCTACATCCGAGTCGTGGACGTGCC	98M11I43M2S1D86M	346	2	36
	GTCCGGCAGTATCTGCTCGATGCCTTCCAGCTTAATAAAGCCAGCCTGCTGATCCGGGATGCCCTGATGCTGGCTCGAACCGGCGGCTTCCTCTCCGCCTCCCCCGCCGCTCTGCGCACCGGGCTCCGCGCCGCCACCCGCGCCAGGAGGGCTCTCCTCGCTAGGAGTGACCTCTCCGTCCGTGATCAGACGCCTTTCCTCGGCTACATCCGAGTCGTGGACGTGCC	142M3D85M	222	1	-
hcn4l	AGGAGAGGAAATCCACGGCAAACCAGCTGCGCAAGTACCTGACCTTGATCTGCTGAGGGTCCAGGATGATTTCTGTACTGTCCTCTTTCACAATCCCCGTGCGGAAGTTCAGCACGAGGTCGACCAGGAAGAAGGTGTCGGAGACCACGTTAAACACTATCCAGGCGGGTGTGTGTTCGTCTTTGAAGAAGGTGATGCCCACGGGGATGATGATCAGGTTGCCCACCATTAGAAG	115M1S89M1S29M	1076	697	671
	AGGAGAGGAAATCCACGGCAAACCAGCTGCGCAAGTACCTGACCTTGATCTGCTGAGGGTCCAGGATGATTTCTGTACTGTCCTCTTTCACAATCCCCGTGCGGAAGTTCAGCACCAGGTCGACCAGGAAGAAGGTGTCGGAGACCACGTTAAACACTATCCAGGCGGGTGTGTGTTCGTCTTTGAAGAAGGTGATGCCCACGGGAATGATGATCAGGTTGCCCACCATTAGAAG	235M	765	38	389
	AGGAGAGGAAATCCACGGCAAACCAGCTGCGCAAGTACCTGACCTTGATCTGCTGAGGGTCCAGGATGATTTCTGTACTGTCCTCTTTCACAATCCCCGTGCGGAAGTTCAGCACGAGGTCGACCAGGAAGAAGGTGTCGGAGACCACGTAACACTATCCAGGCGGGTGTGTGTTCGTCTTTGAAGAAGGTGATGCCCACGGGGATGATGATCAGGTTGCCCACCATTAGAAG	115M1S34M2D53M1S29M	585	18	295

Continued Supplementary Table 2

Orthologue	Sequence	Cigar	Mean Nr reads	Nr alleles	SD reads
hcn4l	AGGAGAGGAAATCCACGGCAAACCAGCTGCGCAAGTACCTGACCTTGATCTGCTGAGGGTCCAGGATGATTTCTG TACTGTCCTCTTTCACAATCCCCGTGCGGAAGTTCAGCACGAGGTCGACCAGGAAGAAGGTGTCGGAGACCAGGC GGGTGTGTGTTCGTCTTTGAAGAAGGTGATGCCCACGGGGATGATGATCAGGTTGCCCACCATTAGAAG	115M1S28M16D45M1S29M	523	9	176
	AGGAGAGGAAATCCACGGCAAACCAGCTGCGCAAGTACCTGACCTTGATCTGCTGAGGGTCCAGGATGATTTCTG TACTGTCCTCTTTCACAATCCCCGTGCGGAAGTTCAGCACGAGGTCGACCAGGAAGAAGGTGTCGGAGACCACGT TTAAACACTATCCAGGCGGGTGTGTGTTCGTCTTTGAAGAAGGTGATGCCCACGGGGATGATGATCAGGTTGCCC ACCATTAGAAG	115M1S33M1I56M1S29M	1218	4	915
	CAGTGAGGAACTTCAGCCCATTCTGGTTCTCCACGGAGCCGTCGGATACACTAGCGGTGCGAGGAGCGCCAGTTC TCCTCAACTGCTCAGTCCACAGCGAGTCTCCTGCCAAGATCGAGTGGAAAAAAGATGGCTCTTTCCTCAGCCTGGC TTCAGATGAGCGCAGACAGGTCCTGGCCGATGGCTCTCTGCTCATCAGCTCAGTGGTGCACTCC	157M1S57M	941	151	691
	CAGTGAGGAACTTCAGCCCATTCTGGTTCTCCACGGAGCCGTGCGAGGAGCGCCAGTTCTCGCCAGTTCTCCTCAA CTGCTCAGTCCACAGCGAGTCTCCTGCCAAGATCGAGTGGAAAAAAGATGGCTCTTTCCTCAGCCTGGCTTCAGAT GAGCGCAGACAGGTCCTGGCCGATGGCTCTCTGCTCATCAGCTCAGTGGTGCACTCC	40M16D10M10I91M1S57M	957	95	545
	CAGTGAGGAACTTCAGCCCATTCTGGTTCTCCACGGAGCCGTCGGATACACGGTGCGAGGAGCGCCAGTTCTCCTC AACTGCTCAGTCCACAGCGAGTCTCCTGCCAAGATCGAGTGGAAAAAAGATGGCTCTTTCCTCAGCCTGGCTTCAG ATGAGCGCAGACAGGTCCTGGCCGATGGCTCTCTGCTCATCAGCTCAGTGGTGCACTCC	50M4D103M1S57M	899	82	475
	CAGTGAGGAACTTCAGCCCATTCTGGTTCTCCACGGAGCCGTGCGAGGAGCGCCAGTTCTCCTCAACTGCTCAGTC CACAGCGAGTCTCCTGCCAAGATCGAGTGGAAAAAAGATGGCTCTTTCCTCAGCCTGGCTTCAGATGAGCGCAGA CAGGTCCTGGCCGATGGCTCTCTGCTCATCAGCTCAGTGGTGCACTCC	40M16D101M1S57M	696	72	413
	CAGTGAGGAACTTCAGCCCATTCTGGTTCTCCACGGAGCCGTCGGATACACGAGGAGCGCCAGTTCTCCTCAACTG CTCAGTCCACAGCGAGTCTCCTGCCAAGATCGAGTGGAAAAAAGATGGCTCTTTCCTCAGCCTGGCTTCAGATGAG CGCAGACAGGTCCTGGCCGATGGCTCTCTGCTCATCAGCTCAGTGGTGCACTCC	50M9D98M1S57M	589	72	305
	CAGTGAGGAACTTCAGCCCATTCTGGTTCTCCACGGAGCCGTCGGTGCGAGGAGCGCCAGTTCTCCTCAACTGCTC AGTCCACAGCGAGTCTCCTGCCAAGATCGAGTGGAAAAAAGATGGCTCTTTCCTCAGCCTGGCTTCAGATGAGCG CAGACAGGTCCTGGCCGATGGCTCTCTGCTCATCAGCTCAGTGGTGCACTCC	42M12D103M1S57M	703	66	359
neo1a	CAGTGAGGAACTTCAGCCCATTCTGGTTCTCCACGGAGCAGTTCTCCTCAACTGCTCAGTCCACAGCGAGTCTCCTG CCAAGATCGAGTGGAAAAAAGATGGCTCTTTCCTCAGCCTGGCTTCAGATGAGCGCAGACAGGTCCTGGCCGATG GCTCTCTGCTCATCAGCTCAGTGGTGCACTCC	38M31D88M1S57M	985	57	521
	CAGTGAGGAACTTCAGCCCATTCTGGTTCTCCACGGAGCCGTCGGATACAGCGGTGCGAGGAGCGCCAGTTCTCC TCAACTGCTCAGTCCACAGCGAGTCTCCTGCCAAGATCGAGTGGAAAAAAGATGGCTCTTTCCTCAGCCTGGCTTC AGATGAGCGCAGACAGGTCCTGGCCGATGGCTCTCTGCTCATCAGCTCAGTGGTGCACTCC	49M3D105M1S57M	960	20	653
	CAGTGAGGAACTTCAGCCCATTCTGGTTCTCCACGGAGCCGTCGGATACGAGGAGCGCCAGTTCTCCTCAACTGCT CAGTCCACAGCGAGTCTCCTGCCAAGATCGAGTGGAAAAAAGATGGCTCTTTCCTCAGCCTGGCTTCAGATGAGC GCAGACAGGTCCTGGCCGATGGCTCTCTGCTCATCAGCTCAGTGGTGCACTCC	48M11D98M1S57M	633	20	415
	CAGTGAGGAACTTCAGCCCATTCTGGTTCTCCACGGAGCCGTCGGATAGCGGTGCGAGGAGCGCCAGTTCTCCTC AACTGCTCAGTCCACAGCGAGTCTCCTGCCAAGATCGAGTGGAAAAAAGATGGCTCTTTCCTCAGCCTGGCTTCAG ATGAGCGCAGACAGGTCCTGGCCGATGGCTCTCTGCTCATCAGCTCAGTGGTGCACTCC	46M5D106M1S57M	1026	19	474
	CAGTGAGGAACTTCAGCCCATTCTGGTTCTCCACGGAGCCGTCGGATTCTCCTCAACTGCTCAGTCCACAGCGAGT CTCCTGCCAAGATCGAGTGGAAAAAAGATGGCTCTTTCCTCAGCCTGGCTTCAGATGAGCGCAGACAGGTCCTGG CCGATGGCTCTCTGCTCATCAGCTCAGTGGTGCACTCC	46M26D85M1S57M	672	16	404
	CAGTGAGGAACTTCAGCCCATTCAGCCCATTCTGGTTCTCCACGGAGCCGTCGGATACATCCATTCAGCGGTGCGA GGAGCGCCAGTTCTCCTCAACTGCTCAGTCCACAGCGAGTCTCCTGCCAAGATCGAGTGGAAAAAAGATGGCTCTT TCCTCAGCCTGGCTTCAGATGAGCGCAGACAGGTCCTGGCCGATGGCTCTCTGCTCATCAGCTCAGTGGTGCACTC C	11M9I39M5I2S105M1S57M	688	14	336
	CAGTGAGGAACTTCAGCCCATTCTGGTTCTCCACGGAGCGCCAGTTCTCCTCAACTGCTCAGTCCACAGCGAGTCTC CTGCCAAGATCGAGTGGAAAAAAGATGGCTCTTTCCTCAGCCTGGCTTCAGATGAGCGCAGACAGGTCCTGGCCG ATGGCTCTCTGCTCATCAGCTCAGTGGTGCACTCC	34M28D95M1S57M	807	11	252

Continued Supplementary Table 2

Orthologue	Sequence	Cigar	Mean Nr reads	Nr alleles	SD reads
neo1a	CAGTGAGGAACTTCAGCCCATTCTGGTTCTCCACGGAGCCGTCGGATACAAAGCGAGGAGCGCCAGTTCTCCTCAACTGCTCAGTCCACAGCGAGTCTCCTGCCAAGATCGAGTGGAAAAAAGATGGCTCTTTCCTCAGCCTGGCTTCAGATGAGCGCAGACAGGTCCTGGCCGATGGCTCTCTGCTCATCAGCTCAGTGGTGCACTCC	50M6D2S99M1S57M	569	10	314
	CAGTGAGGAACTTCAGCCCATTCTGGTTCTCCACGGAGCCGTTCTCCTCAACTGCTCAGTCCACAGCGAGTCTCCTGCCAAGATCGAGTGGAAAAAAGATGGCTCTTTCCTCAGCCTGGCTTCAGATGAGCGCAGACAGGTCCTGGCCGATGGCTCTCTGCTCATCAGCTCAGTGGTGCACTCC	40M31D86M1S57M	1179	9	312
	CAGTGAGGAACTTCAGCCCATTCTGGTTCTCCACGGAGCCGTCGGATACACCAGCGGTGCGAGGAGCGCCAGTTCTCCTCAACTGCTCAGTCCACAGCGAGTCTCCTGCCAAGATCGAGTGGAAAAAAGATGGCTCTTTCCTCAGCCTGGCTTCAGATGAGCGCAGACAGGTCCTGGCCGATGGCTCTCTGCTCATCAGCTCAGTGGTGCACTCC	51M1S105M1S57M	1569	6	1406
	CAGTGAGGAACTTCAGCCCATTCTGGTTCTCCACGGAGCCGTCGGATACACCAGCGCCAGTTCTCCTCAACTGCTCAGTCCACAGCGAGTCTCCTGCCAAGATCGAGTGGAAAAAAGATGGCTCTTTCCTCAGCCTGGCTTCAGATGAGCGCAGACAGGTCCTGGCCGATGGCTCTCTGCTCATCAGCTCAGTGGTGCACTCC	51M1S12D93M1S57M	1010	6	552
	CAGTGAGGAACTTCAGCCCATTCTGGTTCTCCACGGAGCCGTCGGATACACGGTGCGGAGCGGTGCGAGGAGCGCCAGTTCTCCTCAACTGCTCAGTCCACAGCGAGTCTCCTGCCAAGATCGAGTGGAAAAAAGATGGCTCTTTCCTCAGCCTGGCTTCAGATGAGCGCAGACAGGTCCTGGCCGATGGCTCTCTGCTCATCAGCTCAGTGGTGCACTCC	51M6I1S105M1S57M	760	6	543
	CAGTGAGGAACTTCAGCCCATTCTGGTTCTCCACGGAGCCGTCGGAGCGGTGCGAGGAGCGCCAGTTCTCCTCAACTGCTCAGTCCACAGCGAGTCTCCTGCCAAGATCGAGTGGAAAAAAGATGGCTCTTTCCTCAGCCTGGCTTCAGATGAGCGCAGACAGGTCCTGGCCGATGGCTCTCTGCTCATCAGCTCAGTGGTGCACTCC	45M7D105M1S57M	1451	5	663
	CAGTGAGGAACTTCAGCCCATTCTGGTTCTCCACGGAGCCGTCGGATAGTCGGATAGTTCTCCTCAACTGCTCAGTCCACAGCGAGTCTCCTGCCAAGATCGAGTGGAAAAAAGATGGCTCTTTCCTCAGCCTGGCTTCAGATGAGCGCAGACAGGTCCTGGCCGATGGCTCTCTGCTCATCAGCTCAGTGGTGCACTCC	48M2S1M11D3M4D1S87M1S57M	754	5	361
	CAGTGAGGAACTTCAGCCCATTCTGGTTCTCCACGGAGCCGTCGGATACACTAGCGGTGCGAGGAGCGCCAGTTCTCCTCAACTGCTCAGTTCAGACGAACGCAGACAGGTCCTGGCCGATGGCTCTCTGCTCATCAGCTCAGTGGTGCACTCC	160M1S54M	734	4	441
	CAGTGAGGAACTTCAGCCCATTCTGGTTCTCCACGGAGCCGTCCTGGCGAGGAGCGCCAGTTCTCCTCAACTGCTCAGTCCACAGCGAGTCTCCTGCCAAGATCGAGTGGAAAAAAGATGGCTCTTTCCTCAGCCTGGCTTCAGATGAGCGCAGACAGGTCCTGGCCGATGGCTCTCTGCTCATCAGCTCAGTGGTGCACTCC	43M7D2M1S5D99M1S57M	376	2	40
	CAGTGAGGAACTTCAGCCCATTCTGGTTCTCCACGGAGCCGTCGGATGTAGCGGTGCGAGGAGTGTAGCGGTGCGAGGAGCGCCAGTTCTCCTCAACTTCTCAGTCCACAGCGAGTCTCCTGCCAAGATCGAGTGGAAAAAAGATGGCTCTTTCCTCAGCCTGGCTTCAGATGAGCGCAGACAGGTCCTGGCCGATGGCTCTCTGCTCATCAGCTCAGTGGTGCACTCC	47M2S1M14I1S33M1S72M1S57M	1242	1	-
	CAGTGAGGAACTTCAGCCCATTCTGGTTCTCCACTAGCGGTGCGAGGAGCGCCAGTTCTCCTCAACTGCTCAGTCCACAGCGAGTCTCCTGCCAAGATCGAGTGGAAAAAAGATGGCTCTTTCCTCAGCCTGGCTTCAGATGAGCGCAGACAGGTCCTGGCCGATGGCTCTCTGCTCATCAGCTCAGTGGTGCACTCC	31M17D109M1S57M	698	1	-
neo1b	TGGCAGGTCTTCCGCGGTTCCTCAGTCAGCCGGAGGGTGTTTCTGTTCGCAGCGGTGGGACTGAGATGCTGAGCTGTGAGGTGACGGAGGAGCTGGTCCCGTTCACCCGCTGGGACAGAGATGCTGTGGAGCTGGACAGCAGGGTCATTCAGCTGCCCAGCGGAGCTCTGGTCATCAGCAACGCCTCACAGGCTGACGCC	123M6D64M1S12M	1295	155	1734
	TGGCAGGTCTTCCGCGGTTCCTCAGTCAGCCGGAGGGTGTTTCTGTTCGCAGCGGTGGGACTGAGATGCTGAGCTGTGAGGTGACGGAGGAGCTGGTCCCGTTCACCCGCTGGGACAGAGATGCTCGGCTGTGGAGCTGGACAGCAGGGTCATTCAGCTGCCCAGCGGAGCTCTGGTCATCAGCAACGCCTCGCAGGCTGACGCC	128M1D77M	1334	100	1800
	TGGCAGGTCTTCCGCGGTTCCTCAGTCAGCCGGAGGGTGTTTCTGTTCGCAGCGGTGGGACTGAGATGCTGAGCTGTGAGGTGACGGAGGAGCTGGTCCCGTTCACCCGCTGGGACAGAGATGCTCGGCAGCTGGACAGCAGGGTCATTCAGCTGCCCAGCGGAGCTCTGGTCATCAGCAACGCCTCGCAGGCTGACGCC	129M6D71M	1207	87	1570

Continued Supplementary Table 2

Orthologue	Sequence	Cigar	Mean Nr reads	Nr alleles	SD reads
	TGGCAGGTCTTCCGCGGTTCCTCAGTCAGCCGGAGGGTGTTTCTGTTCGCAGCGGTGGGACTGAGATGCTGAGCT GTGAGGTGACGGAGGAGCTGGTCCCGTTCACCCGCTGGGACAGAGATGCTCGGCTCGGCTGTGGAGCTGGACAG CAGGGTCATTCAGCTGCCCAGCGGAGCTCTGGTCATCAGCAACGCCTCGCAGGCTGACGCC	129M4I77M	1430	78	1952
	TGGCAGGTCTTCCGCGGTTCCTCAGTCAGCCGGAGGGTGTTTCTGTTCGCAGCGGTGGGACTGAGATGCTGAGCT GTGAGGTGACGGAGGAGCTGGTCCCGTTCACCCGCTGGGACAGAGATGCTGTGGAGCTGGACAGCAGGGTCATT CAGCTGCCCAGCGGAGCTCTGGTCATCAGCAACGCCTCGCAGGCTGACGCC	123M6D77M	1342	33	2035
	TGGCAGGTCTTCCGCGGTTCCTCAGTCAGCCGGAGGGTGTTTCTGTTCGCAGCGGTGGGACTGAGATGCTGAGCT GTGAGGTGACGGAGGAGCTGGTCCCGTTCACCCGCTGGGACAGAGATGCTCGGCAGCAGGGTCTGGGTCTGGAG CTGGACAGCAGGGTCATTCAGCTGCCCAGCGGAGCTCTGGTCATCAGCAACGCCTCGCAGGCTGACGCC	129M8I3M4I74M	1573	32	2534
	TGGCAGGTCTTCCGCGGTTCCTCAGTCAGCCGGAGGGTGTTTCTGTTCGCAGCGGTGGGACTGAGATGCTGAGCT GTGAGGTGACGGAGGAGCTGGTCCCGTTCACCCGCTGGGACAGAGATGTGGAGCTGGACAGCAGGGTCATTCAG CTGCCCAGCGGAGCTCTGGTCATCAGCAACGCCTCACAGGCTGACGCC	121M9D63M1S12M	1017	27	1531
	TGGCAGGTCTTCCGCGGTTCCTCAGTCAGCCGGAGGGTGTTTCTGTTCGCAGCGGTGGGACTGAGATGCTGAGCT GTGAGGTGACGGAGGAGCTGGTCCCGTTCACCCGCTGGGACAGAGATGCTCGGCCTGTGGAGCTGGACAGCAGG GTCATTCAGCTGCCCAGCGGAGCTCTGGTCATCAGCAACGCCTCGCAGGCTGACGCC	206M	679	24	1019
	TGGCAGGTCTTCCGCGGTTCCTCAGTCAGCCGGAGGGTGTTTCTGTTCGCAGCGGTGGGACTGAGATGCTGAGCT GTGAGGTGACGGAGGAGCTGGTCCCGTTCACCCGCTGGGACAGAGATGCTCTGTGGAGCTGGACAGCAGGGTCA TTCAGCTGCCCAGCGGAGCTCTGGTCATCAGCAACGCCTCGCAGGCTGACGCC	125M4D77M	1884	22	2143
	TGGCAGGTCTTCCGCGGTTCCTCAGTCAGCCGGAGGGTGTTTCTGTTCGCAGCGGTGGGACTGAGATGCTGAGCT GTGAGGTGACGGAGGAGCTGGTCCCGTTCACCCGCTGGGACAGAGATGCTCGGCCTGTGGAGCTGGACAGCAGG GTCATTCAGCTGCCCAGCGGAGCTCTGGTCATCAGCAACGCCTCACAGGCTGACGCC	193M1S12M	347	16	543
neo1b	TGGCAGGTCTTCCGCGGTTCCTCAGTCAGCCGGAGGGTGTTTCTGTTCGCAGCGGTGGGACTGAGATGCTGAGCT GTGAGGTGACGGAGGAGCTGGTCCCGTTCACCCGCTGGGACAGAGATGCTCGGAGCTGGACAGCAGGGTCATTC AGCTGCCCAGCGGAGCTCTGGTCATCAGCAACGCCTCACAGGCTGACGCC	126M7D60M1S12M	345	14	675
	TGGCAGGTCTTCCGCGGTTCCTCAGTCAGCCGGAGGGTGTTTCTGTTCGCAGCGGTGGGACTGAGATGCTGAGCT GTGAGGTGACGGAGGAGCTGGTCCCGTTCACCCGCTGGGACAGAGATGCTCAGCAGGGTCATTCAGCTGCCCAG CGGAGCTCTGGTCATCAGCAACGCCTCACAGGCTGACGCC	125M17D51M1S12M	1504	9	1182
	TGGCAGGTCTTCCGCGGTTCCTCAGTCAGCCGGAGGGTGTTTCTGTTCGCAGCGGTGGGACTGAGATGCTGAGCT GTGAGGTGACGGAGGAGCTGGTCCCGTTCACCCGCTGGGACAGAGGGACATTCAGGACATTCAGCTGCCCAGCG GAGCTCTGGTCATCAGCAACGCCTCGCAGGCTGACGCC	120M19D5M4S2M1S55M	1278	9	1869
	TGGCAGGTCTTCCGCGGTTCCTCAGTCAGCCGGAGGGTGTTTCTGTTCGCAGCGGTGGGACTGAGATGCTGAGCT GTGAGGTGACGGAGGAGCTGGTCCCGTTCACCCGCTGGGACAGGACAGCAGGGTCATTCAGCTGCCCAGCGGAG CTCTGGTCATCAGCAACGCCTCACAGGCTGACGCC	117M22D54M1S12M	1197	2	
	TGGCAGGTCTTCCGCGGTTCCTCAGTCAGCCGGAGGGTGTTTCTGTTCGCAGCGGTGGGACTGAGATGCTGAGCT GTGAGGTGACGGAGGAGCTGGTCCCGTTCACCCGCTGGGACAGAGATGCTCATTCAGATGCTCATGACAGCAGG GTCATTCAGCTGCCCAGCGGAGCTCTGGTCATCAGCAACGCCTCGCAGGCTGACGCC	126M3S1M1S1M2S1M2S1M2S66M	8	2	1
	TGGCAGGTCTTCCGCGGTTCCTCAGTCAGCCGGAGGGTGTTTCTGTTCGCAGCGGTGGGACTGAGATGCTGAGCT GTGAGGTGACGGAGGAGCTGGTCCCGTTCACCCGCTGGGACAGAGATGCTGGACAGCAGGGTCATTCAGCTGCC CAGCGGAGCTCTGGTCATCAGCAACGCCTCGCAGGCTGACGCC	122M14D70M	4	2	1
	TGGCAGGTCTTCCGCGGTTCCTCAGTCAGCCGGAGGGTGTTTCTGTTCGCAGCGGTGGGACTGAGATGCTGAGCT GTGAGGTGACGGAGGAGCTGGTCCCGTTCACCCGCTGGGACAGAGATGCTCGGCAGCTGTGGAGCTGGACAGCA GGGTCATTCAGCTGCCCAGCGGAGCTCTGGTCATCAGCAACGCCTCGCAGGCTGACGCC	129M2I77M	49	1	
	TGGCAGGTCTTCCGCGGTTCCTCAGTCAGCCGGAGGGTGTTTCTGTTCGCAGCGGTGGGACTGAGATGCTGAGCT GTGAGGTGACGGAGGAGCTGGTCCCGTTCACCCGCTGGGACAGAGATCTGTGGAGCTGGACAGCAGGGTCATTC AGCTGCCCAGCGGAGCTCTGGTCATCAGCAACGCCTCGCAGGCTGACGCC	122M7D77M	9	1	

Continued Supplementary Table 2

Orthologue	Sequence	Cigar	Mean Nr reads	Nr alleles	SD reads
quo	CGCAGAGTCTCCTGACCAACATATGACCCAACTTATCACCAGCATGGTCCAAGCAAGACAGCCTCACAAGTCATTCCTCACAGGGCAACCGGATCTCCCTCAGACTGTACTGGGAACTAAGGCCTTACCAGATAAAAGACATCCCTGTCTGAA	6M1S32M1S22M1S90M	997	119	507
	CGCAGAGTCTCCTGACCAACATATGACCCAACTTATCACCAGCATGGTCCAAGCAAGACAGCCTCACAAGTCAACCGGATCTCCCTCAGACTGTACTGGGAACTAAGGCCTTACCAGATAAAAGACATCCCTGTCTGAA	6M1S32M1S22M1S8M14D68M	1117	99	569
	CGCAGAGTCTCCTGACCAACATATGACCCAACTTATCACCAGCATGGTCCAAGCAAGACAGCCTCACAAGTCATTCCTCAACCGGATCTCCCTCAGACTGTACTGGGAACTAAGGCCTTACCAGATAAAAGACATCCCTGTCTGAA	6M1S32M1S22M1S15M7D68M	1175	80	598
	CGCAGAGTCTCCTGACCAACATATGACCCAACTTATCACCAACTTATCACCAGCATGGTCCAAGCAAGACAGCATCACAAGTCATTCCTCAGACTGTACTGGGAACTAAGGCCTTACCAGATAAAAGATATCCCTGTCTGAA	6M1S20M11I12M1S41M3I2S56M1S13M	882	68	903
	CGCAGAGTCTCCTGACCAACATATGACCCAACTTATCACCAGCATGGTCCAAGCAAGACAGCATCACAAGTCATTCCTCCGGATCTCCCTCAGACTGTACTGGGAACTAAGGCCTTACCAGATAAAAGATATCCCTGTCTGAA	6M1S32M1S38M10D51M1S13M	541	57	417
	CGCAGAGTCTCCTGACCAACATATGACCCAACTTATCACCAGCATGGTCCAAGCAAGACAGCATCACAAGTCATTCCTCACAACCGGGCAACCGGATCTCCCTCAGACTGTACTGGGAACTAAGGCCTTACCAGATAAAAGATATCCCTGTCTGAA	6M1S32M1S42M3I57M1S13M	780	55	596
	CGCAGAGTCTCCTGACCAACATATGACCCAACTTATCACCAGCATGGTCCAAGCAAGACAGCCTCACAAGTCATTCCTCACCTCAGACTGTACTGGGAACTAAGGCCTTACCAGATAAAAGACATCCCTGTCTGAA	6M1S32M1S22M1S17M17D56M	1077	38	490
	CGCAGAGTCTCCTGACCAACATATGACCCAACTTATCACCAGCATGGTCCAAGCAAGACAGCCTCACAAGTCATTCCTCACCGGCAACCGGATCTCCCTCAGACTGTACTGGGAACTAAGGCCTTACCAGATAAAAGACATCCCTGTCTGAA	6M1S32M1S22M1S18M1S1D70M	876	30	459
	CGCAGAGTCTCCTGACCAACATATGACCCAACTTATCACCAGCATGGTCCAAGCAAGACAGCATCACAAGTCATTCCTCACAGGGCAACCGGATCTCCCTCAGACTGTACTGGGAACTAAGGCCTTACCAGATAAAAGATATCCCTGTCTGAA	6M1S32M1S99M1S13M	775	30	588
	CGCAGAGTCTCCTGACCAACATATGACCCAACTTATCACCAGCATGGTCCAAGCAAGACAGCATCACAAGTCATTCCTCACAACCGCAACCGGATCTCCCTCAGACTGTACTGGGAACTAAGGCCTTACCAGATAAAAGATATCCCTGTCTGAA	6M1S32M1S42M1S1I1S55M1S13M	822	22	547
	CGCAGAGTCTCCTGACCAACATATGACCCAACTTATCACCAGCATGGTCCAAGCAAGACAGCCTCACAAGTCATTCACAAGTCATTCTCCCTCAGACTGTACTGGGAACTAAGGCCTTACCAGATAAAAGACATCCCTGTCTGAA	6M1S32M1S22M1S11M3D5M1S1M1S2M5D1S60M	1190	21	408
	CGCAGAGTCTCCTGACCAACATATGACCCAACTTATCACCAGCATGGTCCAAGCAAGACAGCCTCACAAGTCATTCCTCATGACGGCAACCGGATCTCCCTCAGACTGTACTGGGAACTAAGGCCTTACCAGATAAAAGACATCCCTGTCTGAA	6M1S32M1S22M1S17M1S1I1M1S70M	1469	20	683
	CGCAGAGTCTCCTGACCAACATATGACCCAACTTATCACCAGCATGGTCCAAGCAAGACAGCCTCACAAGTCATTCCTCACAACCGGATCTCCCTCAGACTGTACTGGGAACTAAGGCCTTACCAGATAAAAGACATCCCTGTCTGAA	6M1S32M1S22M1S17M5D68M	1365	18	561
	CGCAGAGTCTCCTGACCAACATATGACCCAACTTATCACCAGCATGGTCCAAGCAAGACAGCCTCACAAGTCATTCCTCACAAGGGCAACCGGATCTCCCTCAGACTGTACTGGGAACTAAGGCCTTACCAGATAAAAGACATCCCTGTCTGAA	6M1S32M1S22M1S18M1I72M	1602	14	834
	CGCAGAGTCTCCTGACCAACATAATGTACTGGGAACTAAGGCCTTACCAGATAAAAGATATCCCTGTCTGAA	6M1S15M81D1M1S34M1S13M	1070	14	568
	CGCAGAGTCTCCTGACCAACATATGACCCAACTTATCACCAGCATGGTCCAAGCAAGACAGCCTCACAAGTCATTCCGCAACCGGATCTCCCTCAGACTGTACTGGGAACTAAGGCCTTACCAGATAAAAGACATCCCTGTCTGAA	6M1S32M1S22M1S14M7D69M	1063	14	794
	CGCAGAGTCTCCTGACCAACATATGACCCAACTTATCACCAGCATGGTCCAAGCAAGACAGCCTCACTAACAACCGGATCTCCCTCAGACTGTACTGGGAACTAAGGCCTTACCAGATAAAAGACATCCCTGTCTGAA	6M1S32M1S22M1S4M1S1M15D1S68M	876	12	386
	CGCAGAGTCTCCTGACCAACATATGACCCAACTTATCACCAGCATGGTCCAAGCAAGACAGCCTCACAAGTCATTCCTCAACCGGACTCAGGGCAACCGGATCTCCCTCAGACTGTACTGGGAACTAAGGCCTTACCAGATAAAAGACATCCCTGTCTGAA	6M1S32M1S22M1S17M8I73M	950	10	426

Continued Supplementary Table 2

Orthologue	Sequence	Cigar	Mean Nr reads	Nr alleles	SD reads
	CGCAGAGTCTCCTGACCAACATATGACCCAACTTATCACCAGCATGGTCCAAGCAAGACAGCATCACAAGTCATTCCTCAACCGGCAACCGGATCTCCCTCAGACTGTACTGGGAACTAAGGCCTTACCAGATAAAAGATATCCCTGTCTGAA	6M1S32M1S40M3S56M1S13M	618	9	283
	CGCAGAGTCTCCTGACCAACATATGACCCAACTTATCACCAGCATGGTCCAAGCAAGACAGCATCACAAGTCATTCCTCACAAGGGCAACCGGATCTCCCTCAGACTGTACTGGGAACTAAGGCCTTACCAGATAAAAGATATCCCTGTCTGAA	6M1S32M1S41M1I58M1S13M	581	6	250
	CGCAGAGTCTCCTGACCAACATATGACCCAACTTATCACCAGCATGGTCCAAGCAAGACAGCATCACAAGTCATTCCTCACAACCGCAACCGGATCTCCCTCAGACTGTACTGGGAACTAAGGCCTTACCAGATAAAAGACATCCCTGTCTGAA	6M1S32M1S42M1S1I1S69M	145	6	23
	CGCAGAGTCTCCTGACCAACATATGACCCAACTTATCACCAACTTATCACCAGCATGGTCCAAGCAAGACAGCATCACAAGTCATTCCTCACTTGTAGGCAACCGGATCTCCCTCAGACTGTACTGGGAACTAAGGCCTTACCAGATAAAAGACATCCCTGTCTGAA	6M1S20M11I12M1S41M3I2S70M	136	6	89
quo	CGCAGAGTCTCCTGACCAACATATGACCCAACTTATCACCAGCATGGTCCAAGCAAGACAGCATCACAAGTCATTCCTCACCAACCGGATCTCCCTCAGACTGTACTGGGAACTAAGGCCTTACCAGATAAAAGATATCCCTGTCTGAA	6M1S32M1S41M4D54M1S13M	1101	5	323
	CGCAGAGTCTCCTGACCAACATATGACCCAACTTATCACCAGCATGGTCCAAGCAAGACAGCATCACAAGTCATTCCTCACAGGGCAACCGGATCTCCCTCAGACTGTACTGGGAACTAAGGCCTTACCAGATAAAAGACATCCCTGTCTGAA	6M1S32M1S113M	120	4	48
	CGCAGAGTCTCCTGACCAACATATGACCCAACTTATCACCAGCATGGTCCAAGCAAGACAGCATCACAAGTCATTCCTCACAACCGGGCAACCGGATCTCCCTCAGACTGTACTGGGAACTAAGGCCTTACCAGATAAAAGACATCCCTGTCTGAA	6M1S32M1S42M3I71M	107	2	65
	CGCAGAGTCTCCTGACCAACATATGACCCAACTTATCACCAGCATGGTCCAAGCAAGACAGCCTCACAAGTCATTCCTCACCGGCAAGTCATTCGGATCTCCCTCAGACTGTACTGGGAACTAAGGCCTTACCAGATAAAAGACATCCCTGTCTGAA	6M1S32M1S22M1S17M4I2M1S1M1S2M2S64M	1184	1	-
	CGCAGAGTCTCCTGACCAACATAATGTACTGGGAACTAAGGCCTTACCAGATAAAAGACATCCCTGTCTGAA	6M1S15M81D1M1S48M	233	1	-
	CGCAGACTCTCCTGACCAACATATGACCCAACTTATCACAAGCATGGTCCAAGCAAGACAGCATCACAAGTCATTCCTCACAGGGCAACCGGATCTCCCTCAGACTGTACTGGGAACTAAGGCCTTACCAGATAAAAGACATCCCTGTCTGAA	153M	25	1	-
	TCTGATCATCCTAATGAAGCAGAAACTGCTGACCCCTGCGGTGAGGAGAAAATCCAGAGCGCATACCGGGACGGCACATCAGAGAAATGCCACATTGTGATTCAGGGACAGTCAAATCAAGAGGACAGAAG	48M1S22M21D45M1S2M1S11M	985	120	638
	TCTGATCATCCTAATGAAGCAGAAACTGCTGACCCCTGCGGTGAGGAGAAAATCCAGAGCGCATACCGGGACGGTTTGGCTCCAGCAGTGGTCGGCACATCAGAGAAATGCCACATTGTGATTCAGGGACAGTCAAATCAAGAGGACAGAAG	48M1S88M1S2M1S11M	951	78	613
	TCTGATCATCCTAATGAAGCAGAAACTGCTGACCCCTGCGGTGAGGAGAAAATCCAGAGCGCATACCGGGTCGGCACATCAGAGAAATGCCACATTGTGATTCAGGGACAGTCAAATCAAGAGGACAGAAG	48M1S19M21D48M1S2M1S11M	886	63	460
	TCTGATCATCCTAATGAAGCAGAAACTGCTGACCCCTGCGGTGAGGAGAAAATCCAGAGCGCATACCGGGACAGAGAAATGCCACATTGTGATTCAGGGACAGTCAAATCAAGAGGACAGAAG	48M1S22M29D37M1S2M1S11M	1070	62	464
si:dkey-65j6.2	TCTGATCATCCTAATGAAGCAGAAACTGCTGACCCCTGCGGTGAGGAGCAAATCCAGAGCGCATACCGGGACGGTTTGGCTCCAGTGGTCGGCACATCAGAGAAATGCCACATTGTGATTCAGGGACAGTCAAACCAGGAGGACAGAAG	82M3D67M	772	62	333
	TCTGATCATCCTAATGAAGCAGAAACTGCTGACCCCTGCGGTGAGGAGCAAATCCAGAGCGCATACCGGGACGGTTTGGGCACATCAGAGAAATGCCACATTGTGATTCAGGGACAGTCAAACCAGGAGGACAGAAG	78M15D59M	856	59	414
	TCTGATCATCCTAATGAAGCAGAAACTGCTGACCCCTGCGGTGAGGAGCAAATCCAGAGCGCATACCGGGACGGTTTGGCTCATCAGAGAAACACAGAGAAATGGCACATCAGAGAAATGCCACATTGTGATTCAGGGACAGTCAAACCAGGAGGACAGAAG	81M1D2M1S3M1S1M11I3S59M	829	55	457
	TCTGATCATCCTAATGAAGCAGAAACTGCTGACCCCTGCGGTGAGGAGCAAATCCAGAGCGCATACCGGGACGGTTTGGCTCATCAGAGAAATGCCACATTGTGATTCAGGGACAGTCAAACCAGGAGGACAGAAG	81M16D55M	935	35	587

Continued Supplementary Table 2

Orthologue	Sequence	Cigar	Mean Nr reads	Nr alleles	SD reads
	TCTGATCATCCTAATGAAGCAGAAACTGCTGACCCCTGCGGTGAGGAGCAAATCCAGAGCGCATACCGGGACGGTTTGGTCGGCACATCAGAGAAATGCCACATTGTGATTCAGGGACAGTCAAACCAGGAGGACAGAAG	76M12D64M	837	33	470
	TCTGATCATCCTAATGAAGCAGAAACTGCTGACCCCTGCGGTGAGGAGCAAATCCAGAGCGCATACCGGGACGGTTTGGCTCCAGCAGTGGTCGGCACATCAGAGAAATGCCACATTGTGATTCAGGGACAGTCAAACCAGGAGGACAGAAG	152M	564	32	351
	TCTGATCATCCTAATGAAGCAGAAACTGCTGACCCCTGCGGTGAGGAGAAAATCCAGAGCGCATACCGGGACAGTGGTCGGCACATCAGAGAAATGCCACATTGTGATTCAGGGACAGTCAAATCAAGAGGACAGAAG	48M1S22M14D52M1S2M1S11M	964	26	370
	TCTGATCATCCTAATGAAGCAGAAACTGCTGACCCCTGCGGTGAGGAGAAAATCCAGAGCGCATACCGGGACGGTTTGGCTCCAGTGGTCGGCACATCAGAGAAATGCCACATTGTGATTCAGGGACAGTCAAATCAAGAGGACAGAAG	48M1S33M3D52M1S2M1S11M	793	20	426
	TCTGATCATCCTAATGAAGCAGAAACTGCTGACCCCTGCGGTGAGGAGAAAATCCAGAGCGCATACCGGGACGGGACCAGTGGTCGGCACATCAGAGAAATGCCACATTGTGATTCAGGGACAGTCAAATCAAGAGGACAGAAG	48M1S25M1S8D1M1S52M1S2M1S11M	787	19	595
	TCTGATCATCCTAATGAAGCAGAAACTGCTGACCCCTGCGGTGAGGAGAAAATCCAGAGCGCATACCGGGACGGTACATCAGAGAAATGCCACATTGTGATTCAGGGACAGTCAAATCAAGAGGACAGAAG	48M1S26M21D41M1S2M1S11M	1035	18	370
	TCTGATCATCCTAATGAAGCAGAAACTGCTGACCCCTGCGGTGAGGAGAAAATCCAGAGCGCATACCGGGACGGTTTGGGTCGGCACATCAGAGAAATGCCACATTGTGATTCAGGGACAGTCAAATCAAGAGGACAGAAG	48M1S29M11D48M1S2M1S11M	657	17	443
	TCTGATCATCCTAATGAAGCAGAAACTGCTGACCCCTGCGGTGAGGAGAAAATCCAGAGCGCATACCGGGACGGTCGGCACATCAGAGAAATGCCACATTGTGATTCAGGGACAGTCAAATCAAGAGGACAGAAG	48M1S23M17D48M1S2M1S11M	1152	15	331
si:dkey-65j6.2	TCTGATCATCCTAATGAAGCAGAAACTGCTGACCCCTGCGGTGAGGAGCAAATCCAGAGCGCATACCGGGACGGTTTAAAAATAAGGCTAGTGGTCGGCACATCAGAGAAATGCCACATTGTGATTCAGGGACAGTCAAACCAGGAGGACAGAAG	77M8I4M5D66M	584	11	214
	TCTGATCATCCTAATGAAGCAGAAACTGCTGACCCCTGCGGTGAGGAGCAAATCCAGAGCGCATACCGGGACGGCACATCAGAGAAATGCCACATTGTGATTCAGGGACAGTCAAACCAGGAGGACAGAAG	71M21D60M	1110	9	532
	TCTGATCATCCTAATGAAGCAGAAACTGCTGACCCCTGCGGTGAGGAGCAAATCCAGAGCGCATACCGGGACGGCACATCCAGTGGTCGGCACATCAGAGAAATGCCACATTGTGATTCAGGGACAGTCAAACCAGGAGGACAGAAG	74M5S1M5D67M	970	9	382
	TCTGATCATCCTAATGAAGCAGAAACTGCTGACCCCTGCGGTGAGGAGCAAATCCAGAGCGCATACCGGGACGGAAATGCCACATTGTGATTCAGGGACAGTCAAACCAGGAGGACAGAAG	73M31D48M	976	4	130
	TCTGATCATCCTAATGAAGCAGAAACTGCTGACCCCTGCGGTGAGGAGCAAATCCAGAGCGCATACCGGGACGATGTGGTCGGCACATCAGAGAAATGCCACATTGTGATTCAGGGACAGTCAAACCAGGAGGACAGAAG	73M1S1M12D65M	726	4	358
	TCTGATCATCCTAATGAAGCAGAAACTGCTGACCCCTGCGGTGAGGAGAAAATCCAGAGCGCATACCGGGACGGTATGGCACATCAGAGAAATGCCACATTGTGATTCAGGGACAGTCAAATCAAGAGGACAGAAG	48M1S26M1S1M16D44M1S2M1S11M	1411	3	177
	TCTGATCATCCTAATGAAGCAGAAACTGCTGACCCCTGCGGTGAGGAGCAAATCCAGAGCGCATACCGGGTCGGCACATCAGAGAAATGCCACATTGTGATTCAGGGACAGTCAAACCAGGAGGACAGAAG	68M21D63M	913	3	550
	TCTGATCATCCTAATGAAGCAGAAACTGCTGACCCCTGCGGTGAGGAGCAAATCCAGAGCGCATACCGGGACGGTATGGTCGACATCAGAGAAATGCCACATTGTGATTCAGGGACAGTCAAACCAGGAGGACAGAAG	75M12D1S6M2D56M	834	3	128
	TCTGATCATCCTAATGAAGCAGAAACTGCTGACCCCTGCGGTGAGGAGAAAATCCAGAGCGCATACCGGGACGGTTTGGTCGAACAGTGGTCGGCACATCAGAGAAATGCCACATTGTGATTCAGGGACAGTCAAATCAAGAGGACAGAAG	48M1S30M1D2M1S1M1S52M1S2M1S11M	562	1	-
	TCTGATCATCCTAATGAAGCAGAAACTGCTGACCCCTGCGGTGAGGAGAAAATCCAGAGCGCATACCGGGACATCAGAGAAATGCCACATTGTGATTCAGGGACAGTCAAATCAAGAGGACAGAAG	48M1S21M26D41M1S2M1S11M	558	1	-
dclk1b	ATGTGTGTGGATCAATTGAGCCTTACAAGATGCAGGAATATACTAAAAACGTCAACCCTAACTGGTCGGTCAACATGAGAACCACTGCCGGAGCAAAACCGCCCACCTCTCTGGCCAGTGCCAAGGGCGGGTCTATAGAAACCAAGGATAACAGGGATTTCATCCGACCCAAACTGGTGACCATAATCCGTAGCGGGGTAAAGCCTCGGAAAGCCATCCGAATCCTTCTCAACAA	235M	1638	377	1281

Continued Supplementary Table 2

Orthologue	Sequence	Cigar	Mean Nr reads	Nr alleles	SD reads
dclk1b	ATGTGTGTGGATCAATTGAGCCTTACAAGATGCAGGAATATACTAAAAACGTCAACCCTAACTGGTCGGTCAACAT GAGAACCACTGCCGGAGCAAAACCGCCCACCTCTCTGGCCAGTGCCAAGGGCGGGTCTATAGAAACCAAGGATAA CAGGGATTTCATCCGACCCAAACTGGTGACCATAATCCGTAGTGGGGTAAAGCCTCGGAAAGCCATCCGAATCCTT CTCAACAA	193M1S41M	1078	102	877
galnt10chr21	GCGTAACGTGGGCACTGGGCTGTGTGTGGAGAGCAAACACTTCTCCTCCGGGTCCCCGATCCGCCTGGAACCATG CCTGAGGAGCCGCGGAGAGCCCAGCTGGAGCCACGGGCAGGTGAGACACGCACCGCTAACAGCGCTAGCACTAG AGACACACACTGCTAACTGCTAATA	174M	1246	198	994
	GCGTAACGTGGGCACTGGGCTGTGTGTGGAGAGCAAACACTTCTCCTCTGGGTCCCCGATCCGCCTGGAACCATG CCTGAGGAGCCGCGGAGAGCCCAGCTGGAGCCACGGGCAGGTGAGACACGCACCGCTAACAGCGCTAGCACTAG AGACACACACTGCTAACTGCTAATA	48M1S125M	952	364	1044
galnt10scaff	GTGGGCACTGGGCTGTGTGTGGAGAGCAAACACTTCTCCTCTGGGTCCCCGATCCGCCTGGAACCATGCCTGAGG AGCCGCGGAGAGCCCAGCTGGAGCCACGGGCAGGTGAGACACGCACCGCTAACAGCGCTAGCACTAGAGACACA CACTGCTAACTGCTAATATGGCTAACTCTGTGTGTGTGTGTGTGTGTGTGTGTGTGT	41M1S135M12D27M	272	326	207
	GTGGGCACTGGGCTGTGTGTGGAGAGCAAACACTTCTCCTCCGGGTCCCCGATCCGCCTGGAACCATGCCTGAGG AGCCGCGGAGAGCCCAGCTGGAGCCACGGGCAGGTGAGACACGCACCGCTAACAGCGCTAGCACTAGAGACACA CACTGCTAACTGCTAATATGGCTAACTCTCTGTGTGTGTGTGTGTGTGTGTGTGTGTGTGTGTGTGTGT	216M	148	187	106
	GTGGGCACTGGGCTGTGTGTGGAGAGCAAACACTTCTCCTCTGGGTCCCCGATCCGCCTGGAACCATGCCTGAGG AGCCGCGGAGAGCCCAGCTGGAGCCACGGGCAGGTGAGACACGCACCGCTAACAGCGCTAGCACTAGAGACACA CACTGCTAACTGCTAATATGGCTAACTCTGTGTGTGTGTGTGTGTGTGTGTGTGTGT	41M1S135M14D25M	157	136	94
	GTGGGCACTGGGCTGTGTGTGGAGAGCAAACACTTCTCCTCTGGGTCCCCGATCCGCCTGGAACCATGCCTGAGG AGCCGCGGAGAGCCCAGCTGGAGCCACGGGCAGGTGAGACACGCACCGCTAACAGCGCTAGCACTAGAGACACA CACTGCTAACTGCTAATATGGCTAACTCTGTGTGTGTGTGTGTGTGTGTGTGTGTGTGTGTGTGTGTGT	41M1S135M8D31M	147	82	107
	GTGGGCACTGGGCTGTGTGTGGAGAGCAAACACTTCTCCTCCGGGTCCCCGATCCGCCTGGAACCATGCCTGAGG AGCCGCGGAGAGCCCAGCTGGAGCCACGGGCAGGTGAGACACGCACCGCTAACAGCGCTAGCACTAGAGACACA CACTGCTAACTGCTAATATGGCTAACTCTCTGTGTGTGTGTGTGTGTGTGTGTGTGTGTGTGTGTGTGTGT	214M2N	136	13	127
	GTGGGCACTGGGCTGTGTGTGGAGAGCAAACACTTCTCCTCTGGGTCCCCGATCCGCCTGGAACCATGCCTGAGG AGCCGCGGAGAGCCCAGCTGGAGCCACGGGCAGGTGAGACACGCACCGCTAACAGCGCTAGCACTAGAGACACA CACTGCTAACTGCTAATATGGCTAACTCTGTGTGTGTGTGTGTGTGTGTGTGTGTGTGTGTGTGTGTGTGT	41M1S135M10D29M	4	2	1

All unique sequences identified for targeted orthologues and their respective alignment report string (Cigar). Mean number of reads, the number of alleles the cigar was found in and the standard deviation (SD) are reported. Cigar letters: M=match, D=deletion, I=insertion, S=substitution. The genes *quo* and *si:dkey-65j6.2* are orthologues of the human *KIAA1755*.

Supplementary Table 3: Unique variants and affected transcripts

Orthologue	Chr	ENSDARG	Affected transcripts	Start (bp)	End (bp)	Mutation	Annotation	Base pair change	VEP impact	Nr affected alleles
				40 856 888	40 856 893	AAGGCG/-	inframe deletion	-6	moderate	75
				40 856 893	40 856 895	GAA/-	inframe deletion	-3	moderate	3
				40 856 894	40 856 894	A/-	frameshift variant	-1	high	69
gngt1	19	ENSDARG00000035798	ENSDART00000051950 ENSDART00000139083	40 856 895	40 856 895	A/T	missense variant	0	moderate	3
				40 856 895	40 856 897	AGA/TTT	missense variant	0	moderate	69
				40 856 897	40 856 896	-/TAAC	stop gained,frameshift variant	4	high	2
				40 856 897	40 856 899	ATG/CCA	missense variant	0	moderate	2
				10 888 933	10 888 953	GACATGAATGTCCGCACAGAG/-	inframe deletion	-21	moderate	19
				10 888 944	10 888 944	C/A	synonymous variant	0	low	42
				10 888 945	10 888 944	-/CAGCTGATG	inframe insertion	9	moderate	42
				10 888 946	10 888 950	GCACA/-	frameshift variant	-5	high	3
				10 888 946	10 888 952	GCACAGA/-	frameshift variant	-7	high	15
				10 888 946	10 888 953	GCACAGAG/-	frameshift variant	-8	high	40
				10 888 947	10 888 947	C/T	synonymous variant	0	low	42
				10 888 948	10 888 948	A/C	missense variant	0	moderate	4
				10 888 948	10 888 954	ACAGAGG/-	frameshift variant	-7	high	11
syt10	4	ENSDARG00000045750	ENSDART00000136049	10 888 949	10 888 958	CAGAGGACGG/-	frameshift variant	-10	high	4
				10 888 950	10 888 949	-/GGGAATGG	frameshift variant	8	high	42
				10 888 950	10 888 949	-/A	frameshift variant	1	high	44
				10 888 950	10 888 950	A/G	synonymous variant	0	low	11
				10 888 951	10 888 951	G/T	stop gained	0	high	42
				10 888 952	10 888 951	-/CAT	stop gained,protein altering variant	3	high	11
				10 888 952	10 888 952	A/-	frameshift variant	-1	high	42
				10 888 952	10 888 953	AG/CA	missense variant	0	moderate	11
				10 888 959	10 888 960	CA/TG	missense variant	0	moderate	4
				28 638 811	28 638 822	CCCACCGCACCT/-	inframe deletion	-12	moderate	1
				28 638 820	28 638 820	C/-	frameshift variant	-1	high	24
rgs6	20	ENSDARG00000015627	ENSDART00000135513 ENSDART00000184779	28 638 820	28 638 821	CC/-	frameshift variant	-2	high	7
				28 638 820	28 638 822	CCT/-	inframe deletion	-3	moderate	4
				28 638 824	28 638 824	G/A	stop gained	0	high	4
				28 638 837	28 638 836	-/CTGAGCCATG	frameshift variant	10	high	4
				1 143 637	1 143 644	ACCCGCGG/-	frameshift variant	-8	high	13
				1 143 638	1 143 638	C/T	missense variant	0	moderate	16
				1 143 641	1 143 641	G/A	missense variant	0	moderate	9
				1 143 643	1 143 643	G/-	frameshift variant	-1	high	11
				1 143 643	1 143 644	GG/CA	missense variant	0	moderate	2
				1 143 643	1 143 646	GGCT/-	frameshift variant	-4	high	9
				1 143 644	1 143 643	-/CCGCCAC	frameshift variant	7	high	16
hcn4	18	ENSDARG00000061685	ENSDART00000136140 ENSDART00000189186	1 143 644	1 143 644	G/C	missense variant	0	moderate	75
				1 143 644	1 143 646	GCT/-	inframe deletion	-3	moderate	1
				1 143 645	1 143 644	-/CTCTC	frameshift variant	5	high	15
				1 143 645	1 143 644	-/GCC	protein altering variant	3	moderate	2
				1 143 645	1 143 645	C/-	frameshift variant	-1	high	2
				1 143 646	1 143 645	-/GCCA	frameshift variant	4	high	48
				1 143 646	1 143 646	T/C	synonymous variant	0	low	48
				1 143 652	1 143 651	-/AGCTCC	inframe insertion	6	moderate	15

Continued Supplementary Table 3

Orthologue	Chr	ENSDARG	Affected transcripts	Start (bp)	End (bp)	Mutation	Annotation	Base pair change	VEP impact	Nr affected alleles
hcn4l	25	ENSDARG00000074419	ENSDART00000088249 ENSDART00000148940	29 273 086	29 273 101	CCACGTTAAACACTAT/-	frameshift variant	-16	high	9
				29 273 091	29 273 090	-/T	frameshift variant	1	high	4
				29 273 092	29 273 093	TA/-	frameshift variant	-2	high	18
				53 879 228	53 879 244	CACGGAGCCGTCGGATA/-	frameshift variant	-17	high	1
				53 879 231	53 879 258	GGAGCCGTCGGATACACTAGCGGTGCGA/-	frameshift variant	-28	high	11
				53 879 235	53 879 265	CCGTCGGATACACTAGCGGTGCGAGGAGCGC/-	frameshift variant	-31	high	57
				53 879 237	53 879 252	GTCGGATACACTAGCG/-	frameshift variant	-16	high	157
				53 879 237	53 879 267	GTCGGATACACTAGCGGTGCGAGGAGCGCCA/-	frameshift variant	-31	high	9
				53 879 239	53 879 250	CGGATACACTAG/-	inframe deletion	-12	moderate	66
				53 879 240	53 879 246	GGATACA/-	frameshift variant	-7	high	2
				53 879 242	53 879 248	ATACACT/-	frameshift variant	-7	high	5
				53 879 243	53 879 247	TACAC/-	frameshift variant	-5	high	17
				53 879 243	53 879 268	TACACTAGCGGTGCGAGGAGCGCCAG/-	frameshift variant	-26	high	16
				53 879 244	53 879 245	AC/GT	missense variant	0	moderate	1
				53 879 245	53 879 246	CA/GT	missense variant	0	moderate	5
				53 879 245	53 879 255	CACTAGCGGTG/-	frameshift variant	-11	high	20
				53 879 246	53 879 248	ACT/-	inframe deletion	-3	moderate	20
neo1a	7	ENSDARG00000102855	ENSDART00000158160 ENSDART00000163261 ENSDART00000164768 ENSDART00000181629	53 879 247	53 879 246	-/GCGGTGCGAGGAGT	frameshift variant	14	high	1
				53 879 247	53 879 246	-/TCCAT	frameshift variant	5	high	14
				53 879 247	53 879 247	C/G	missense variant	0	moderate	1
				53 879 247	53 879 248	CT/TC	missense variant	0	moderate	14
				53 879 247	53 879 250	CTAG/-	frameshift variant	-4	high	82
				53 879 247	53 879 252	CTAGCG/-	inframe deletion	-6	moderate	10
				53 879 247	53 879 255	CTAGCGGTG/-	inframe deletion	-9	moderate	69
				53 879 248	53 879 247	-/GGTGCG	protein altering variant	6	moderate	6
				53 879 248	53 879 248	T/G	missense variant	0	moderate	6
				53 879 248	53 879 248	T/C	missense variant	0	moderate	10
				53 879 248	53 879 258	TAGCGGTGCGA/-	frameshift variant	-11	high	5
				53 879 249	53 879 249	A/G	synonymous variant	0	low	2
				53 879 249	53 879 260	AGCGGTGCGAGG/-	inframe deletion	-12	moderate	5
				53 879 250	53 879 254	GCGGT/-	frameshift variant	-5	high	2
				53 879 253	53 879 254	GT/AA	missense variant	0	moderate	10
				53 879 262	53 879 265	GCGC/-	frameshift variant	-4	high	5
				53 879 263	53 879 262	-/CGCCAGTTCT	frameshift variant	10	high	89
				53 879 266	53 879 266	C/T	missense variant	0	moderate	5

Continued Supplementary Table 3

Orthologue	Chr	ENSDARG	Affected transcripts	Start (bp)	End (bp)	Mutation	Annotation	Base pair change	VEP impact	Nr affected alleles
				2 899 719	2 899 719	C/-	frameshift variant	-1	high	65
				2 899 722	2 899 721	-/GGTC	frameshift variant	4	high	18
				2 899 719	2 899 718	-/TCGG	frameshift variant	4	high	51
				2 899 710	2 899 728	ATGCTCGGCCTGTGGAGCT/-	frameshift variant	-19	high	7
				2 899 718	2 899 724	CCTGTGG/-	frameshift variant	-7	high	9
				2 899 716	2 899 719	GGCC/-	frameshift variant	-4	high	15
				2 899 708	2 899 729	AGATGCTCGGCCTGTGGAGCTG/-	frameshift variant	-22	high	1
				2 899 715	2 899 728	CGGCCTGTGGAGCT/-	frameshift variant	-14	high	2
				2 899 712	2 899 718	GCTCGGC/-	frameshift variant	-7	high	1
				2 899 719	2 899 718	-/AGCAGGGT	frameshift variant	8	high	18
neo1b	25	ENSDARG00000075100	ENSDART00000115280	2 899 719	2 899 718	-/AG	frameshift variant	2	high	1
				2 899 716	2 899 732	GGCCTGTGGAGCTGGAC/-	frameshift variant	-17	high	5
				2 899 719	2 899 724	CTGTGG/-	inframe deletion	-6	moderate	59
				2 899 713	2 899 721	CTCGGCCTG/-	inframe deletion	-9	moderate	18
				2 899 722	2 899 723	TG/AT	missense variant	0	moderate	2
				2 899 725	2 899 726	AG/CT	missense variant	0	moderate	2
				2 899 734	2 899 737	GCAG/TTCA	missense variant	0	moderate	7
				2 899 728	2 899 729	TG/AT	missense variant	0	moderate	2
				2 899 716	2 899 718	GGC/ATT	missense variant	0	moderate	2
				2 899 715	2 899 720	CGGCCT/-	inframe deletion	-6	moderate	108
				2 899 740	2 899 740	T/A	missense variant	0	moderate	7
				2 899 720	2 899 720	T/A	synonymous variant	0	low	2

Continued Supplementary Table 3

Orthologue	Chr	ENSDARG	Affected transcripts	Start (bp)	End (bp)	Mutation	Annotation	Base pair change	VEP impact	Nr affected alleles
				2 051 654	2 051 734	ATGACCCAACTTATCACAAGCATGGTCCAAGCAAGACAGCATCAC AAGTCATTCCTCACAGGGCAACCGGATCTCCCTCAG/-	inframe deletion	-81	moderate	13
				2 051 699	2 051 699	A/T	stop gained	0	high	10
				2 051 701	2 051 715	GTCATTCCTCACAGG/-	inframe deletion	-15	moderate	10
				2 051 703	2 051 716	CATTCCTCACAGGG/-	frameshift variant	-14	high	61
				2 051 706	2 051 708	TCC/-	inframe deletion	-3	moderate	17
				2 051 709	2 051 715	TCACAGG/-	frameshift variant	-7	high	9
				2 051 710	2 051 716	CACAGGG/-	frameshift variant	-7	high	53
				2 051 710	2 051 719	CACAGGGCAA/-	frameshift variant	-10	high	51
				2 051 712	2 051 711	-/CCGG	frameshift variant	4	high	1
				2 051 712	2 051 711	-/ACCGGACT	frameshift variant	8	high	7
				2 051 712	2 051 712	C/T	missense variant	0	moderate	15
				2 051 712	2 051 714	CAG/ACC	missense variant	0	moderate	9
				2 051 712	2 051 716	CAGGG/-	frameshift variant	-5	high	14
			ENSDART00000109679	2 051 712	2 051 728	CAGGGCAACCGGATCTC/-	frameshift variant	-17	high	23
			ENSDART00000153568	2 051 713	2 051 712	-/G	frameshift variant	1	high	15
quo	6	ENSDARG00000073684	ENSDART00000187502	2 051 713	2 051 712	-/A	frameshift variant	1	high	19
			ENSDART00000187544	2 051 713	2 051 712	-/TTG	stop gained,inframe insertion	3	high	70
			ENSDART00000191165	2 051 713	2 051 713	A/C	synonymous variant	0	low	22
				2 051 713	2 051 714	AG/TA	missense variant	0	moderate	70
				2 051 713	2 051 716	AGGG/-	frameshift variant	-4	high	4
				2 051 714	2 051 713	-/ACC	inframe insertion	3	moderate	51
				2 051 714	2 051 714	G/-	frameshift variant	-1	high	22
				2 051 714	2 051 714	G/A	missense variant	0	moderate	40
				2 051 714	2 051 714	G/C	missense variant	0	moderate	15
				2 051 715	2 051 714	-/C	frameshift variant	1	high	22
				2 051 715	2 051 715	G/C	missense variant	0	moderate	22
				2 051 716	2 051 716	G/T	synonymous variant	0	low	18
				2 051 716	2 051 716	G/A	synonymous variant	0	low	10
				2 051 719	2 051 720	AC/TT	missense variant	0	moderate	1
				2 051 719	2 051 723	ACCGG/-	frameshift variant	-5	high	17
				2 051 724	2 051 724	A/T	missense variant	0	moderate	17
				2 051 736	2 051 736	C/A	missense variant	0	moderate	13

Continued Supplementary Table 3

Orthologue	Chr	ENSDARG	Affected transcripts	Start (bp)	End (bp)	Mutation	Annotation	Base pair change	VEP impact	Nr affected alleles
				43 213 133	43 213 153	GGACGGTTTGGCTCCAGCAGT/-	inframe deletion	-21	moderate	62
				43 213 135	43 213 160	ACGGTTTGGCTCCAGCAGTGGTCGGC/-	frameshift variant	-26	high	1
				43 213 136	43 213 149	CGGTTTGGCTCCAG/-	frameshift variant	-14	high	21
				43 213 136	43 213 156	CGGTTTGGCTCCAGCAGTGGT/-	inframe deletion	-21	moderate	101
				43 213 136	43 213 164	CGGTTTGGCTCCAGCAGTGGTCGGCACAT/-	frameshift variant	-29	high	50
				43 213 137	43 213 153	GGTTTGGCTCCAGCAGT/-	frameshift variant	-17	high	15
				43 213 138	43 213 138	G/A	missense variant	0	moderate	4
				43 213 138	43 213 168	GTTTGGCTCCAGCAGTGGTCGGCACATCAGA/-	frameshift variant	-31	high	3
				43 213 139	43 213 139	T/G	synonymous variant	0	low	18
				43 213 139	43 213 143	TTTGG/CACAT	missense variant	0	moderate	9
				43 213 140	43 213 140	T/A	missense variant	0	moderate	3
				43 213 140	43 213 147	TTGGCTCC/-	frameshift variant	-8	high	18
				43 213 140	43 213 151	TTGGCTCCAGCA/-	inframe deletion	-12	moderate	7
				43 213 140	43 213 160	TTGGCTCCAGCAGTGGTCGGC/-	inframe deletion	-21	moderate	12
				43 213 141	43 213 152	TGGCTCCAGCAG/-	inframe deletion	-12	moderate	32
				43 213 142	43 213 141	-/AAAAATAA	frameshift variant	8	high	7
			ENSDART00000158832	43 213 142	43 213 157	GGCTCCAGCAGTGGTC/-	frameshift variant	-16	high	3
			ENSDART00000164262	43 213 143	43 213 153	GCTCCAGCAGT/-	frameshift variant	-11	high	13
*si:dkey-65j6..*23		ENSDARG00000103586	ENSDART00000186065	43 213 143	43 213 157	GCTCCAGCAGTGGTC/-	inframe deletion	-15	moderate	57
			ENSDART00000190315	43 213 144	43 213 144	C/-	frameshift variant	-1	high	1
			ENSDART00000193300	43 213 145	43 213 149	TCCAG/-	frameshift variant	-5	high	9
				43 213 146	43 213 146	C/-	frameshift variant	-1	high	41
				43 213 146	43 213 150	CCAGC/-	frameshift variant	-5	high	7
				43 213 146	43 213 161	CCAGCAGTGGTCGGCA/-	frameshift variant	-16	high	34
				43 213 147	43 213 147	C/G	missense variant	0	moderate	1
				43 213 147	43 213 149	CAG/-	inframe deletion	-3	moderate	69
				43 213 149	43 213 149	G/T	missense variant	0	moderate	41
				43 213 149	43 213 149	G/C	missense variant	0	moderate	18
				43 213 149	43 213 149	G/A	missense variant	0	moderate	1
				43 213 152	43 213 152	G/A	missense variant	0	moderate	3
				43 213 153	43 213 153	T/A	missense variant	0	moderate	41
				43 213 155	43 213 154	-/AAACACAGAGA	frameshift variant	11	high	41
				43 213 155	43 213 157	GTC/AAT	missense variant	0	moderate	41
				43 213 159	43 213 160	GC/-	frameshift variant	-2	high	3

The predicted impact of unique CRISPR-Cas9 induced mutations on protein function was assessed using Ensembl's Variant Effect Predictor (VEP). An allele- and target-specific dosage score was subsequently calculated for each larva by weighting the mutation with the highest predicted impact by a factor 0.33, 0.66, or 1 for mutations with a low, moderate or high predicted impact, respectively. Modification of expression was only observed for transcripts of genes located near the targeted gene. Start and end coordinates are based on GRCz11. The genes *quo* and *si:dkey-65j6.2* are orthologues of the human *KIAA1755*.

Supplementary Table 4: Mutant allele frequencies

	Nr mutated alleles						Expected nr mutated alleles			
Gene	**0**	**1**	**2**	**Missing**	**Sample call rate**	**Mutant allele freq**	**0**	**1**	**2**	**P_{HWE}**
gngt1	234	130	12	5	0.987	0.205	238	122	16	2.33E-01
syt10	192	130	54	5	0.987	0.316	176	163	38	9.82E-05
rgs6	344	34	1	2	0.995	0.047	344	34	1	8.69E-01
hcn4	266	100	9	6	0.984	0.157	266	99	9	9.12E-01
hcn4l	349	29	1	2	0.995	0.041	349	30	1	6.32E-01
neo1a	19	113	240	9	0.976	0.797	15	120	236	2.39E-01
neo1b	14	12	277	78	0.795	0.934	1	37	264	3.24E-32
quo	55	42	281	3	0.992	0.799	15	121	241	4.69E-37
si:dkey-65j6.2	22	60	295	4	0.990	0.862	7	90	280	1.34E-10

Number of larvae with 0, 1 and 2 mutated alleles, as well as the number of larvae with a missing call. *P*-value for a Hardy-Weinberg equilibrium (HWE) exact test, considering a ±30 bp window around the CRISPR targeted site as a single locus (*P*<2.9E-3 is significant after Bonferroni correction). Larvae with more than two missing genotypes were excluded from the statistical analysis (i.e. n_total=381). The genes *quo* and *si:dkey-65j6.2* are orthologues of the human *KIAA1755*.

Supplementary Table 5: Transcript-specific association analysis for heart rate variability and heart rate

					Model 1					Model 2				
Age	**Outcome**	**n**	**Factor**	**Gene**	**Effect size**	**SE**	**LCI**	**UCI**	**P**	**Effect size**	**SE**	**LCI**	**UCI**	**P**
				gngt1	-0.080	0.131	-0.337	0.176	5.41E-01	-0.009	0.116	-0.236	0.217	9.37E-01
				syt10	-0.003	0.088	-0.176	0.170	9.75E-01	-0.006	0.078	-0.159	0.147	9.38E-01
				rgs6	-0.477	0.213	-0.895	-0.060	2.49E-02	-0.376	0.188	-0.745	-0.008	4.53E-02
				hcn4	-0.043	0.116	-0.271	0.184	7.08E-01	0.023	0.105	-0.182	0.227	8.29E-01
				hcn4l	0.096	0.182	-0.259	0.452	5.96E-01	0.148	0.162	-0.169	0.465	3.59E-01
			fixed	*neo1a*	0.110	0.118	-0.121	0.341	3.49E-01	0.138	0.107	-0.072	0.348	1.99E-01
2	Heart rate	234		*neo1b*	0.006	0.120	-0.230	0.241	9.61E-01	0.062	0.107	-0.149	0.272	5.65E-01
				quo	-0.076	0.084	-0.240	0.088	3.64E-01	0.000	0.076	-0.149	0.149	1.00E+00
				si:dkey-65j6.2	0.059	0.108	-0.152	0.270	5.84E-01	0.167	0.097	-0.023	0.358	8.49E-02
				time of day	0.459	0.042	0.378	0.541	2.07E-28	0.579	0.040	0.500	0.658	1.55E-46
				HRV (in SD)	-	-	-	-	-	-0.424	0.052	-0.526	-0.321	6.06E-16
				intercept	-1.353	0.280	-1.902	-0.805	1.33E-06	-2.148	0.285	-2.706	-1.590	4.47E-14
			random	variation by batch	0.031	0.233	0.000	66000	-	0.098	0.097	0.014	0.680	-
				residual	0.810	0.038	0.738	0.889	-	0.712	0.034	0.649	0.781	-
				gngt1	0.155	0.141	-0.120	0.431	2.69E-01	0.112	0.124	-0.131	0.354	3.66E-01
				syt10	-0.027	0.096	-0.214	0.161	7.78E-01	-0.032	0.084	-0.197	0.132	7.00E-01
				rgs6	0.270	0.230	-0.181	0.720	2.41E-01	0.031	0.204	-0.370	0.431	8.80E-01
				hcn4	0.246	0.129	-0.008	0.499	5.75E-02	0.209	0.114	-0.015	0.432	6.71E-02
				hcn4l	0.083	0.200	-0.309	0.476	6.78E-01	0.110	0.176	-0.236	0.455	5.34E-01
			fixed	*neo1a*	0.011	0.139	-0.261	0.283	9.37E-01	0.046	0.123	-0.195	0.288	7.06E-01
2	HRV	234		*neo1b*	0.172	0.133	-0.088	0.432	1.94E-01	0.172	0.117	-0.057	0.400	1.41E-01
				quo	0.116	0.097	-0.074	0.307	2.32E-01	0.072	0.086	-0.097	0.241	4.03E-01
				si:dkey-65j6.2	0.188	0.121	-0.050	0.426	1.21E-01	0.221	0.107	0.012	0.431	3.87E-02
				time of day	0.296	0.047	0.204	0.388	2.80E-10	0.526	0.050	0.428	0.624	5.05E-26
				Heart rate (in SD)	-	-	-	-	-	-0.513	0.062	-0.636	-0.391	2.07E-16
				intercept	-1.718	0.381	-2.466	-0.970	6.68E-06	-2.362	0.353	-3.054	-1.670	2.20E-11
			random	variation by batch	0.310	0.128	0.138	0.697	-	0.306	0.119	0.143	0.657	-
				residual	0.869	0.041	0.792	0.952	-	0.763	0.036	0.696	0.837	-
				gngt1	0.001	0.123	-0.240	0.242	9.96E-01	0.068	0.101	-0.130	0.266	5.01E-01
				syt10	-0.018	0.083	-0.181	0.145	8.31E-01	-0.049	0.068	-0.183	0.085	4.75E-01
				rgs6	-0.170	0.179	-0.520	0.181	3.43E-01	-0.062	0.147	-0.351	0.227	6.75E-01
				hcn4	0.338	0.106	0.130	0.545	1.44E-03	0.157	0.089	-0.016	0.331	7.58E-02
				hcn4l	-0.035	0.202	-0.430	0.360	8.63E-01	0.024	0.166	-0.301	0.350	8.83E-01
			fixed	*neo1a*	-0.139	0.115	-0.365	0.087	2.27E-01	-0.090	0.095	-0.277	0.097	3.47E-01
5	Heart rate	285		*neo1b*	0.136	0.131	-0.121	0.392	3.00E-01	0.083	0.108	-0.128	0.294	4.42E-01
				quo	0.011	0.089	-0.165	0.186	9.04E-01	0.022	0.074	-0.123	0.168	7.62E-01
				si:dkey-65j6.2	-0.076	0.113	-0.297	0.146	5.02E-01	0.030	0.094	-0.153	0.214	7.48E-01
				time of day	0.410	0.051	0.310	0.509	6.80E-16	0.565	0.044	0.479	0.651	5.89E-38
				HRV (in SD)	-	-	-	-	-	-0.524	0.045	-0.613	-0.435	7.90E-31
				intercept	-1.243	0.421	-2.069	-0.417	3.17E-03	-1.858	0.406	-2.654	-1.063	4.70E-06
			random	variation by batch	0.509	0.181	0.253	1.023	-	0.615	0.206	0.319	1.186	-
				residual	0.845	0.036	0.778	0.918	-	0.694	0.029	0.639	0.754	-
				gngt1	0.125	0.133	-0.136	0.386	3.47E-01	0.130	0.109	-0.084	0.344	2.35E-01
				syt10	-0.063	0.089	-0.237	0.111	4.76E-01	-0.066	0.074	-0.211	0.078	3.69E-01
				rgs6	0.231	0.192	-0.145	0.608	2.29E-01	0.100	0.159	-0.212	0.412	5.30E-01
				hcn4	-0.286	0.112	-0.506	-0.066	1.09E-02	-0.129	0.096	-0.317	0.059	1.78E-01
				hcn4l	0.056	0.211	-0.358	0.470	7.90E-01	0.080	0.179	-0.272	0.431	6.56E-01
			fixed	*neo1a*	0.117	0.118	-0.114	0.348	3.22E-01	0.035	0.103	-0.167	0.237	7.34E-01
5	HRV	285		*neo1b*	-0.014	0.139	-0.286	0.257	9.17E-01	0.002	0.116	-0.226	0.231	9.83E-01
				quo	0.072	0.092	-0.107	0.251	4.31E-01	0.053	0.080	-0.103	0.209	5.06E-01
				si:dkey-65j6.2	0.243	0.119	0.010	0.476	4.08E-02	0.173	0.101	-0.024	0.370	8.59E-02
				time of day	0.241	0.050	0.143	0.339	1.51E-06	0.521	0.050	0.423	0.620	2.36E-25
				Heart rate (in SD)	-	-	-	-	-	-0.601	0.053	-0.705	-0.498	3.75E-30
				intercept	-1.293	0.366	-2.010	-0.575	4.14E-04	-1.981	0.386	-2.738	-1.223	2.97E-07
			random	variation by batch	0.145	0.092	0.042	0.500	-	0.477	0.170	0.237	0.959	-
				residual	0.915	0.039	0.842	0.994	-	0.751	0.032	0.692	0.816	-

Associations of heart rate variability (HRV) and heart rate with the number of mutated alleles across the nine orthologues, weighted by their predicted effect on protein function. Associations were examined for the main transcript of each targeted zebrafish orthologue using hierarchical linear models (xtmixed in Stata), using inverse-normally transformed outcomes, so effect sizes and SEs can be interpreted as z-score units. Associations were adjusted for time of day and the weighted number of mutated alleles in the other genes as fixed factors, with larvae nested in batches (random factor). Additionally, Model 2 includes mutual adjustment of heart rate and HRV. The genes *quo* and *si:dkey-65j6.2* are orthologues of the human *KIAA1755*.

Supplementary Table 6: Transcript-specific association analyses for body size

			2dpf						5dpf					
Outcome	**Factor**	**Gene**	**n**	**Effect size**	**SE**	**LCI**	**UCI**	**P**	**n**	**Effect size**	**SE**	**LCI**	**UCI**	**P**
		gngt1		-0.120	0.115	-0.346	0.106	2.97E-01		0.043	0.115	-0.182	0.268	7.05E-01
		syt10		0.147	0.080	-0.009	0.303	6.54E-02		0.095	0.076	-0.053	0.243	2.09E-01
		rgs6		-0.444	0.179	-0.795	-0.094	1.31E-02		-0.467	0.181	-0.822	-0.113	9.65E-03
		hcn4		-0.131	0.101	-0.330	0.067	1.96E-01		0.080	0.094	-0.104	0.265	3.95E-01
		hcn4l		0.126	0.200	-0.265	0.518	5.28E-01		-0.075	0.192	-0.452	0.301	6.95E-01
	fixed	*neo1a*		-0.029	0.110	-0.244	0.185	7.89E-01		-0.136	0.108	-0.347	0.076	2.09E-01
Length		*neo1b*	332	0.075	0.122	-0.163	0.314	5.37E-01	242	0.045	0.127	-0.205	0.294	7.26E-01
		quo		-0.008	0.083	-0.171	0.156	9.27E-01		-0.026	0.082	-0.186	0.134	7.52E-01
		si:dkey-65j6.2		0.045	0.107	-0.165	0.254	6.77E-01		-0.087	0.105	-0.293	0.119	4.08E-01
		time of day		0.111	0.042	0.029	0.193	7.88E-03		0.091	0.047	-0.001	0.183	5.25E-02
		intercept		-0.490	0.371	-1.216	0.237	1.86E-01		-0.131	0.449	-1.011	0.750	7.71E-01
	random	variation by batch		0.395	0.129	0.208	0.748	-		0.689	0.227	0.361	1.315	-
		residual		0.897	0.035	0.830	0.968	-		0.703	0.032	0.643	0.770	-
		gngt1		0.025	0.110	-0.190	0.240	8.20E-01		-0.091	0.137	-0.360	0.178	5.08E-01
		syt10		0.052	0.076	-0.096	0.201	4.89E-01		0.048	0.090	-0.129	0.225	5.99E-01
		rgs6		-0.031	0.168	-0.361	0.299	8.55E-01		-0.462	0.223	-0.899	-0.024	3.86E-02
		hcn4		-0.022	0.096	-0.210	0.167	8.22E-01		-0.090	0.110	-0.305	0.126	4.14E-01
		hcn4l		0.066	0.188	-0.303	0.435	7.25E-01		0.097	0.222	-0.338	0.531	6.63E-01
	fixed	*neo1a*		0.208	0.105	0.002	0.414	4.76E-02		-0.032	0.125	-0.277	0.214	8.01E-01
Dorsal area		*neo1b*	322	0.003	0.117	-0.226	0.232	9.81E-01	234	-0.139	0.154	-0.441	0.163	3.66E-01
		quo		0.052	0.080	-0.105	0.210	5.16E-01		0.267	0.095	0.081	0.452	4.92E-03
		si:dkey-65j6.2		-0.184	0.103	-0.386	0.019	7.50E-02		-0.274	0.123	-0.515	-0.034	2.54E-02
		time of day		-0.052	0.040	-0.131	0.026	1.89E-01		-0.072	0.053	-0.176	0.032	1.74E-01
		intercept		-0.049	0.365	-0.765	0.668	8.94E-01		0.428	0.406	-0.369	1.225	2.92E-01
	random	variation by batch		0.437	0.138	0.236	0.810	-		0.300	0.129	0.130	0.696	-
		residual		0.842	0.033	0.779	0.910	-		0.824	0.039	0.751	0.903	-
		gngt1		0.052	0.124	-0.192	0.295	6.76E-01		-0.172	0.119	-0.405	0.060	1.47E-01
		syt10		0.086	0.087	-0.084	0.255	3.24E-01		-0.007	0.082	-0.167	0.153	9.30E-01
		rgs6		-0.063	0.182	-0.419	0.293	7.27E-01		-0.074	0.175	-0.417	0.269	6.72E-01
		hcn4		-0.137	0.106	-0.344	0.070	1.95E-01		-0.115	0.102	-0.314	0.084	2.57E-01
		hcn4l		0.053	0.208	-0.354	0.460	7.99E-01		0.195	0.200	-0.196	0.586	3.29E-01
	fixed	*neo1a*		0.235	0.112	0.015	0.454	3.61E-02		-0.034	0.122	-0.272	0.204	7.80E-01
Lateral area		*neo1b*	300	-0.051	0.127	-0.300	0.199	6.89E-01	258	-0.138	0.148	-0.428	0.151	3.48E-01
		quo		0.139	0.088	-0.033	0.312	1.13E-01		0.262	0.092	0.080	0.443	4.66E-03
		si:dkey-65j6.2		-0.248	0.111	-0.466	-0.030	2.57E-02		-0.402	0.117	-0.632	-0.173	5.79E-04
		time of day		-0.047	0.044	-0.134	0.040	2.91E-01		-0.074	0.050	-0.172	0.023	1.35E-01
		intercept		-0.001	0.355	-0.697	0.695	9.97E-01		0.595	0.415	-0.217	1.408	1.51E-01
	random	variation by batch		0.265	0.104	0.123	0.570	-		0.440	0.154	0.221	0.876	-
		residual		0.908	0.038	0.837	0.985	-		0.796	0.035	0.729	0.868	-
		gngt1		0.088	0.110	-0.129	0.304	4.27E-01		-0.187	0.129	-0.441	0.066	1.47E-01
		syt10		0.052	0.076	-0.097	0.202	4.93E-01		-0.023	0.083	-0.186	0.141	7.87E-01
		rgs6		0.093	0.174	-0.249	0.435	5.93E-01		-0.042	0.180	-0.394	0.310	8.13E-01
		hcn4		-0.014	0.096	-0.203	0.174	8.80E-01		0.017	0.102	-0.182	0.217	8.64E-01
		hcn4l		-0.033	0.185	-0.395	0.330	8.59E-01		0.092	0.229	-0.357	0.541	6.87E-01
	fixed	*neo1a*		0.314	0.103	0.113	0.515	2.23E-03		0.033	0.117	-0.196	0.262	7.76E-01
Volume		*neo1b*	299	-0.062	0.111	-0.279	0.154	5.73E-01	199	0.105	0.143	-0.176	0.386	4.64E-01
		quo		0.153	0.078	0.000	0.305	4.98E-02		0.150	0.091	-0.028	0.328	9.82E-02
		si:dkey-65j6.2		-0.239	0.100	-0.435	-0.042	1.74E-02		-0.398	0.116	-0.626	-0.170	6.23E-04
		time of day		-0.065	0.040	-0.144	0.015	1.10E-01		-0.075	0.052	-0.177	0.027	1.50E-01
		intercept		-0.153	0.355	-0.849	0.544	6.67E-01		0.198	0.448	-0.679	1.075	6.58E-01
	random	variation by batch		0.427	0.136	0.229	0.796	-		0.572	0.196	0.292	1.120	-
		residual		0.806	0.033	0.743	0.874	-		0.718	0.037	0.650	0.794	-

Associations were analyzed for the main transcript of each targeted zebrafish orthologue using hierarchical linear models (xtmixed in Stata) using inverse-normally transformed outcomes, so effect sizes and SEs can be interpreted as z-score units. Associations were adjusted for time of day and for the weighted number of mutated alleles in the other genes as fixed factors, with larvae nested in batches (random factor). The genes *quo* and *si:dkey-65j6.2* are orthologues of the human *KIAA1755*.

Supplementary Table 7: Comparison of larvae with two vs. zero functionally knocked alleles for heart rate variability and heart rate

				Model 1					Model 2				
Gene	**Age**	**n**	**Outcome**	**Effect size**	**SE**	**LCI**	**UCI**	**P**	**Effect size**	**SE**	**LCI**	**UCI**	**P**
syt10	2	146	Heart rate	-0.115	0.199	-0.506	0.276	5.64E-01	-0.103	0.176	-0.449	0.243	5.59E-01
			HRV	-0.073	0.205	-0.475	0.329	7.22E-01	-0.128	0.182	-0.485	0.229	4.82E-01
	5	180	Heart rate	-0.184	0.189	-0.555	0.187	3.31E-01	-0.198	0.152	-0.496	0.101	1.95E-01
			HRV	-0.066	0.191	-0.440	0.308	7.30E-01	-0.133	0.157	-0.441	0.174	3.96E-01
hcn4	2	183	Heart rate	0.695	0.358	-0.006	1.396	5.20E-02	0.674	0.309	0.068	1.280	2.93E-02
			HRV	0.148	0.399	-0.634	0.930	7.11E-01	0.520	0.344	-0.153	1.194	1.30E-01
	5	212	Heart rate	1.208	0.321	0.579	1.836	1.66E-04	0.444	0.278	-0.100	0.988	1.10E-01
			HRV	-1.349	0.338	-2.010	-0.687	6.48E-05	-0.759	0.294	-1.335	-0.182	9.91E-03
neo1a	2	70	Heart rate	0.102	0.294	-0.473	0.677	7.28E-01	0.216	0.264	-0.302	0.734	4.15E-01
			HRV	0.029	0.343	-0.643	0.702	9.32E-01	0.094	0.317	-0.527	0.714	7.67E-01
	5	93	Heart rate	0.166	0.274	-0.372	0.704	5.45E-01	0.113	0.247	-0.371	0.597	6.47E-01
			HRV	0.089	0.286	-0.473	0.650	7.57E-01	0.140	0.249	-0.348	0.628	5.75E-01
neo1b	2	80	Heart rate	0.153	0.262	-0.360	0.667	5.58E-01	0.225	0.243	-0.251	0.701	3.55E-01
			HRV	0.292	0.308	-0.312	0.896	3.43E-01	0.332	0.290	-0.236	0.901	2.52E-01
	5	89	Heart rate	0.025	0.325	-0.612	0.661	9.40E-01	-0.073	0.276	-0.614	0.469	7.92E-01
			HRV	0.053	0.333	-0.600	0.706	8.74E-01	-0.092	0.289	-0.658	0.474	7.50E-01
quo	2	170	Heart rate	-0.104	0.178	-0.454	0.245	5.58E-01	0.006	0.167	-0.321	0.332	9.73E-01
			HRV	0.227	0.206	-0.176	0.631	2.70E-01	0.150	0.193	-0.228	0.528	4.36E-01
	5	214	Heart rate	-0.065	0.192	-0.441	0.310	7.34E-01	0.012	0.163	-0.308	0.332	9.40E-01
			HRV	0.240	0.193	-0.139	0.618	2.14E-01	0.203	0.177	-0.144	0.550	2.52E-01
si:dkey-65j6.2	2	60	Heart rate	-0.110	0.226	-0.552	0.332	6.27E-01	0.027	0.216	-0.397	0.452	8.99E-01
			HRV	0.291	0.298	-0.294	0.876	3.29E-01	0.224	0.281	-0.327	0.775	4.25E-01
	5	67	Heart rate	0.111	0.298	-0.473	0.695	7.08E-01	0.160	0.275	-0.378	0.698	5.60E-01
			HRV	0.364	0.350	-0.322	1.051	2.98E-01	0.395	0.328	-0.248	1.038	2.29E-01

Associations of heart rate variability (HRV) and heart rate by comparison of embryos with two functionally knocked alleles with wildtypes. Associations were examined for the main transcript of each targeted zebrafish orthologue using hierarchical linear models (xtmixed in Stata), using inverse-normally transformed outcomes, so effect sizes and SEs can be interpreted as z-score units. In model 1, heart rate and HRV are not mutually adjusted for each other. Associations were adjusted for time of day and the weighted number of mutated alleles in the other genes as fixed factors, with larvae nested in batches (random factor). Model 2 includes additional mutual adjustment of heart rate and HRV. The genes *quo* and *si:dkey-65j6.*2 are orthologues of the human *KIAA1755*.

Supplementary Table 8: Transcript-specific association analysis for dichotomous cardiac outcomes

Age	Outcome	n controls	n cases	Gene	OR	LCI	UCI	P
				gngt1	0.951	0.387	2.336	9.12E-01
				syt10	1.447	0.792	2.642	2.30E-01
				rgs6	0.855	0.193	3.799	8.37E-01
				hcn4	2.644	1.402	4.986	2.66E-03
				neo1a	1.165	0.499	2.717	7.24E-01
				neo1b	1.694	0.434	6.604	4.48E-01
2	SA arrest	248	36	*quo*	0.764	0.404	1.442	4.06E-01
				si:dkey-65j6.2	0.750	0.327	1.720	4.97E-01
				time of day	1.117	0.829	1.506	4.66E-01
				intercept	0.008	0.000	0.414	1.64E-02
				Batch 4	5.656	0.523	61.178	1.54E-01
				Batch 2	11.656	1.342	101.224	2.60E-02
				Batch 3	5.798	0.665	50.571	1.12E-01
				Batch 1	7.540	0.770	73.835	8.27E-02
				gngt1	1.163	0.494	2.740	7.29E-01
				syt10	1.467	0.810	2.654	2.06E-01
				rgs6	0.788	0.175	3.553	7.57E-01
				hcn4	2.749	1.461	5.171	1.71E-03
				neo1a	1.176	0.507	2.731	7.06E-01
				neo1b	2.445	0.658	9.080	1.82E-01
				quo	0.746	0.401	1.389	3.56E-01
2	SA pause	297	39	*si:dkey-65j6.2*	0.755	0.339	1.685	4.93E-01
				time of day	1.147	0.856	1.539	3.59E-01
				intercept	0.004	0.000	0.185	4.77E-03
				Batch 2	14.723	1.714	126.443	1.42E-02
				Batch 3	5.507	0.633	47.917	1.22E-01
				Batch 4	4.948	0.457	53.573	1.88E-01
				Batch 1	7.380	0.755	72.106	8.57E-02
				Batch 5	0.890	0.042	18.778	9.40E-01
				gngt1	0.309	0.037	2.572	2.77E-01
				syt10	0.236	0.050	1.128	7.05E-02
				rgs6	1.049	0.068	16.223	9.73E-01
				hcn4	2.460	0.680	8.899	1.70E-01
				hcn4l	0.937	0.086	10.181	9.58E-01
				neo1a	0.897	0.190	4.232	8.91E-01
				neo1b	1.561	0.162	15.023	7.00E-01
5	SA pause	321	9	*quo*	0.672	0.221	2.043	4.84E-01
				si:dkey-65j6.2	3.533	0.421	29.662	2.45E-01
				time of day	1.066	0.514	2.209	8.64E-01
				intercept	0.016	0.000	7.788	1.90E-01
				Batch 1	0.240	0.011	5.447	3.70E-01
				Batch 3	0.214	0.015	3.049	2.55E-01
				Batch 5	0.213	0.005	8.956	4.18E-01
				Batch 2	0.703	0.073	6.750	7.60E-01

Associations of cardiac outcomes with the number of mutated alleles across the nine orthologues, weighted by their predicted effect on protein function. At 2 and 5 days post fertilization (dpf), associations were analyzed using logistic regression for outcomes where number of observed cases and genotype frequency allowed. Associations were adjusted for time of day and for the weighted number of mutated alleles in the other genes as fixed factors. The genes *quo* and *si:dkey-65j6.2* are orthologues of the human *KIAA1755*.

Supplementary Table 9: Comparison of larvae with two vs. zero functionally knocked alleles for body size

		2dpf						5dpf					
Gene	**Outcome**	**n**	**Effect size**	**SE**	**LCI**	**UCI**	**P**	**n**	**Effect size**	**SE**	**LCI**	**UCI**	**P**
syt10	Length	208	0.207	0.174	-0.135	0.548	2.35E-01	153	0.174	0.182	-0.182	0.530	3.38E-01
	Dorsal area	200	0.022	0.174	-0.320	0.363	9.01E-01	145	0.101	0.204	-0.299	0.501	6.20E-01
	Lateral area	182	0.002	0.200	-0.390	0.393	9.93E-01	155	-0.122	0.193	-0.501	0.257	5.28E-01
	Volume	186	-0.028	0.173	-0.366	0.311	8.73E-01	128	-0.170	0.201	-0.564	0.224	3.98E-01
hcn4	Length	241	0.026	0.306	-0.573	0.625	9.33E-01	177	0.130	0.291	-0.439	0.700	6.54E-01
	Dorsal area	233	-0.020	0.309	-0.626	0.586	9.49E-01	171	0.440	0.319	-0.185	1.065	1.67E-01
	Lateral area	217	0.154	0.321	-0.475	0.783	6.31E-01	183	0.300	0.326	-0.339	0.940	3.57E-01
	Volume	216	0.264	0.303	-0.330	0.858	3.83E-01	141	0.474	0.280	-0.075	1.024	9.06E-02
neo1a	Length	107	-0.188	0.263	-0.703	0.328	4.75E-01	77	-0.317	0.317	-0.939	0.305	3.17E-01
	Dorsal area	104	0.707	0.246	0.224	1.189	4.08E-03	75	0.242	0.340	-0.424	0.907	4.76E-01
	Lateral area	97	-0.072	0.280	-0.621	0.476	7.96E-01	84	0.202	0.356	-0.496	0.901	5.70E-01
	Volume	94	0.516	0.266	-0.005	1.037	5.23E-02	69	-0.164	0.261	-0.676	0.347	5.29E-01
neo1b	Length	117	0.241	0.311	-0.369	0.851	4.38E-01	76	0.378	0.339	-0.286	1.042	2.64E-01
	Dorsal area	112	-0.056	0.296	-0.635	0.523	8.49E-01	72	-0.206	0.430	-1.050	0.637	6.32E-01
	Lateral area	106	0.343	0.336	-0.315	1.001	3.07E-01	74	0.209	0.394	-0.564	0.982	5.96E-01
	Volume	110	0.170	0.284	-0.386	0.726	5.49E-01	62	0.181	0.373	-0.550	0.913	6.27E-01
quo	Length	241	-0.115	0.182	-0.471	0.241	5.27E-01	180	0.078	0.171	-0.256	0.413	6.46E-01
	Dorsal area	235	0.238	0.178	-0.110	0.587	1.80E-01	175	0.545	0.210	0.133	0.957	9.52E-03
	Lateral area	223	0.244	0.198	-0.144	0.632	2.18E-01	188	0.394	0.212	-0.021	0.809	6.30E-02
	Volume	218	0.331	0.174	-0.010	0.671	5.70E-02	146	0.175	0.197	-0.211	0.560	3.75E-01
si:dkey-65j6.2	Length	80	0.221	0.325	-0.416	0.858	4.96E-01	53	-0.107	0.345	-0.782	0.569	7.57E-01
	Dorsal area	78	-0.110	0.266	-0.631	0.412	6.80E-01	51	-0.566	0.317	-1.188	0.056	7.45E-02
	Lateral area	74	-0.489	0.295	-1.067	0.089	9.72E-02	57	-0.622	0.389	-1.384	0.139	1.09E-01
	Volume	75	-0.300	0.262	-0.813	0.212	2.51E-01	44	-0.732	0.338	-1.395	-0.070	3.03E-02

Associations with body size by comparison of embryos with two functionally knocked alleles with wildtypes. Associations were analyzed for the main transcript of each targeted zebrafish orthologue using hierarchical linear models (xtmixed in Stata) using inverse-normally transformed outcomes, so effect sizes and SEs can be interpreted as z-score units. Associations were adjusted for time of day and for the weighted number of mutated alleles in the other genes as fixed factors, with larvae nested in batches (random factor). The genes *quo* and *si:dkey-65j6.2* are orthologues of the human *KIAA1755*.

Supplementary Table 10: Comparison of larvae with two vs. zero functionally knocked alleles for cardiac traits at 2dpf

Gene	Outcome	n controls	n cases	OR	LCI	UCI	P
syt10	SA arrest	141	36	3.480	0.789	15.347	9.95E-02
	SA pause	183	39	3.451	0.792	15.043	9.92E-02
hcn4	SA arrest	149	36	3.666	0.655	20.525	1.39E-01
	SA pause	150	39	3.667	0.633	21.249	1.47E-01
neo1a	SA arrest	72	36	1.200	0.148	9.717	8.65E-01
	SA pause	72	39	1.200	0.148	9.717	8.65E-01
quo	SA arrest	150	36	0.553	0.136	2.239	4.06E-01
	SA pause	190	39	0.513	0.132	1.993	3.35E-01
si:dkey-65j6.2	SA arrest	47	36	0.145	0.009	2.389	1.77E-01
	SA pause	47	39	0.145	0.009	2.389	1.77E-01

Associations of cardiac outcomes by comparison of embryos with two functionally knocked alleles and wildtypes. Associations were analyzed using logistic regression for outcomes where number of observed cases and genotype frequency allowed. Associations were adjusted for time of day and for the weighted number of mutated alleles in the other genes as fixed factors. The genes *quo* and *si:dkey-65j6.2* are orthologues of the human *KIAA1755*.